agriculture

MDPI

Article

Next-Generation Biofertilizers: Nanoparticle-Coated Plant Growth-Promoting Bacteria Biofertilizers for Enhancing Nutrient Uptake and Wheat Growth

Anagha Karunakaran [1], Yaraa Fathima [1], Pallavi Singh [1], Rahul Beniwal [1], Jyoti Singh [2] and Wusirika Ramakrishna [1,*]

[1] Department of Biochemistry, Central University of Punjab, VPO Ghudda, Punjab 151401, India; anaghahkarun00@gmail.com (A.K.); yara.fathima33@gmail.com (Y.F.); pallaviswarajsingh@gmail.com (P.S.); beniwal127@gmail.com (R.B.)

[2] Department of Applied Agriculture, Central University of Punjab, VPO Ghudda, Punjab 151401, India

* Correspondence: rk.wusirika@cup.edu.in or wusirika@gmail.com; Tel.: +91-8999795748

Abstract: Contemporary agricultural practices rely heavily on synthetic fertilizers to provide essential nutrients for crops, contributing to diminished soil fertility and environmental pollution. An innovative solution lies in the strategic combination of nanoparticles and biofertilizers, as a unique and environmentally friendly technology, enhancing soil enzyme activity and the availability of essential plant nutrients. The goal of this study was to show the efficacy of this technology and identify the best combination of nanoparticles and PGPB for plant growth promotion, nutrient uptake, and soil health. This study investigated the efficacy of nanobiofertilizers generated by combining two plant growth-promoting bacteria (PGPB), (*Bacillus* sp.) CP4 and AHP3, along with mesoporous silica nanoparticles (MS NPs), zinc oxide nanoparticles (ZnO NPs), and copper oxide nanoparticles (CuO NPs) in different combinations. A greenhouse study employing two wheat varieties, NABI MG11 (black wheat) and HD3086, was conducted. There were 15 treatments, including treatments consisting of only bacteria, treatments consisting of the combination of nanoparticles and nanobiofertilizers, and 1 control treatment, and each treatment had three replicates. In evaluating plant growth characteristics, the synergy between ZnO NPs and CP4 demonstrated the most favorable outcomes in terms of overall plant growth and various traits. Similarly, MS NPs, in conjunction with both PGPB, exhibited enhancements in plant growth traits, including fresh weight, chlorophyll content, proline levels, and nitrogen content. Over half of the combination treatments with nanoparticles and PGPB did not show a significant improvement in plant growth promotion traits and soil health when compared to nanoparticles alone. The findings of this study underscore the potential of nanobiofertilizers as an innovative and robust tool for promoting sustainable agriculture.

Keywords: nanoparticles; nanobiofertilizer; ZnO; nutrients; plant growth

Citation: Karunakaran, A.; Fathima, Y.; Singh, P.; Beniwal, R.; Singh, J.; Ramakrishna, W. Next-Generation Biofertilizers: Nanoparticle-Coated Plant Growth-Promoting Bacteria Biofertilizers for Enhancing Nutrient Uptake and Wheat Growth. *Agriculture* **2024**, *14*, 517. https://doi.org/10.3390/agriculture14040517

Academic Editor: Dongyang Liu

Received: 3 February 2024
Revised: 20 March 2024
Accepted: 22 March 2024
Published: 23 March 2024

1. Introduction

The tremendous increase in the world population has put forward the great challenge of providing sufficient food products to fed entire communities. To meet this emerging demand in the agricultural sector, pesticides and chemical fertilizers have been used extensively, paving the way for enhanced yields in the production of different crops, leading to a surge in public health hazards, environmental pollution, and a decline in soil fertility [1]. Biofertilizers have emerged as a key alternative for sustainable agricultural practice, which entails the application of beneficial plant growth-promoting microorganisms, including advantageous bacteria and fungi [2,3]. Endophytic plant growth-promoting bacteria (PGPB) invade the leaves, flowers, or interior tissues of the host plant, whereas rhizospheric bacteria are free-living, soil-associated bacteria that establish a symbiotic relationship with plant roots [4].

Biofertilizers maintain the nutrient levels and fertility of the soil through the regulation of different pathways and processes, including phosphate solubilization, nitrogen fixation, the production of siderophores, the release of different plant growth regulators such as IAA, 1-aminocyclopropane-1-carboxylate (ACC) deaminase production, and antibiotic production [3,5,6]. Primarily, a high percentage of the fertilizers applied to the soil, ranging from 20% to 70%, could be lost, and plants only use 10% to 50% of the total fertilizer applied [7,8]. This critical concern demands a new approach that would provide increased shelf-lives and stability for biofertilizers to improve their efficiency.

Bacillus spp. interact with plants in a variety of ways to promote plant growth. Certain *Bacillus* strains have genes for the manufacture of cyclic lipopeptides, which are biosurfactants that promote effective root colonization, the creation of biofilms, and the production of biocontrol compounds that suppress the growth of fungi such as fengycins and iturins [9,10]. Additionally, some strains of *B. subtilis* produce siderophores, which aid in the chelation of iron from the soil and increase the plant's capacity to synthesize photosynthetic substances like heme and chlorophyll [11]. In a previous study, a *Bacillus subtilis* (CP4) treatment exhibited the highest levels for yield-related parameters (average number of grains per spike, thousand-grain weight, and total tillers per plant in wheat) [12]. In addition, wheat variety HD3086, treated with *Bacillus subtilis* (CP4) and arbuscular mycorrhizal fungi (AMF), experience a rise in iron levels to about 25 mg kg^{-1}. Wheat grain proline content significantly increased when *B. subtilis* (CP4) and *Bacillus* sp. (AHP3) were administered alone and together, which is indicative of the extent to which they stabilized the osmotic potential. CP4 increased organic carbon and soil microbial enzymatic activity, reduced pH and electrical conductivity, and enhanced plant growth and biofortification.

Recently, the use of nanotechnology in agriculture has been explored through the study of the precision and efficacy of nanoparticles (NPs) with one or more dimensions in the order of 100 nm or less [13]. Due to their distinct optical properties, high capacity for absorption, high surface-to-volume ratio, and regulated release kinetics, they are favored as probable plant growth promoters and plant protectors. Bacterial priming involves the pre-exposure of bacterial cells to specific stimuli such as nanoparticles or other stressors, resulting in a more robust and efficient response when encountering subsequent challenges. There are several commercially available nanofertilizer preparations for nitrogen (e.g., IFFCO Nano Urea, IFFCO, New Delhi, India), phosphorus (e.g., TAG Nano Phos, SK Organic Farms, Chennai, India), potassium (e.g., NanoMax Potash, JU Agri Sciences, Noida, India), zinc (e.g., Geolife Nano Zn, Geolife Agritech India Ltd., Mumbai, India), and calcium (e.g., Nano Calcium Chelated) [14]. The combination of nanoparticles and biofertilizers has led to the emergence of nanobiofertilizers, where biofertilizers are encapsulated in appropriate nanoparticles [15]. Nanobiofertilizers provide an abated and controlled release of nutrients for a prolonged period at different crop growth stages, along with enhanced nutrient use efficiency, which improves yields. This approach imparts increased shelf-life and stability to the biofertilizer; increases the dissolution of insoluble nutrients present in the soil, along with its solubility; and is price-effective, less time-consuming, and ecologically safe [16]. Through both direct and indirect associations, PGPB work synergistically to increase the soil's ability to retain moisture and plant nutrients while enriching the microbial community [17]. They upregulate the genes that make stress-related proteins, osmolytes, and antioxidants and reduce the damage that ROS induces in plants by augmenting hormonal synthesis and the activity of membrane transporters [18,19].

The specificities and interactions between microorganisms and NPs are mostly determined by the surface charge on the broad distinct surface area of NPs and different chemical groups. Nanoparticles' induction of hydrophobic regions on the cell membrane of bacteria or their adherence to hydrophobic surfaces in the bacteria leads to agglomeration and interaction between bacteria and NPs [20]. A nanoparticle can be synthesized from a single element, such as silver, or by incorporating oxides (TiO_2, SiO_2, ZnO) [21]. Biomolecules interacting with NP include lipopolysaccharide (LPS), lipoteichoic acid (LTA), proteins, and phospholipids present on the bacterial surface [22]. Bacterial cells adhere to nanomate-

rial surfaces through diverse mechanisms, including molecular monolayers composed of proteins, polysaccharides, and/or glycoproteins [23,24]. These adsorbed organic molecules can potentially serve as nutrients for bacteria or alter the surface chemistry to enhance bacterial adherence. Nanomaterials can confer several advantages. For instance, zinc oxide nanoparticles (ZnO NPs) have been shown to enhance siderophore production, likely due to ion release within the bacterium. In a previous study, the application of ZnO NPs to wheat and maize resulted in an increase in the activity of alpha-amylase, along with a slight increase in plant length, biomass, and photosynthetic pigments.

Copper oxide nanoparticles (CuO NPs), when added to soil, promote the development of wheat (*Triticum aestivum*) plants by increasing IAA synthesis in the PGPB, improving nitrogen fixation, enhancing microbial community health, and reducing denitrification processes [25,26]. Higher nitrate levels in the rhizosphere were shown to be correlated with an increased expression of genes involved in nitrogen fixation in [27]. The foliar application of CuO NPs at a concentration of 500 μg mL^{-1} to watermelon plants was associated with both pathogen suppression and higher yield due to the upregulation of the polyphenyl oxide (PPO) genes and pathogenicity-related 1 (PR1) genes [28].

Silica NPs improved the strength and physical resilience of plant cell walls, providing further defense against the invasion of anthophagous insects and phytopathogens [29–31]. In maize, the viability and population of PGPB increased in the soil and also the nitrogen, phosphorus, and potassium (NPK) content, leading to the improved germination of maize seeds in the presence of 50 nm silica nanoparticles [32]. The hydration characteristics of silica NP surfaces make them more attractive to bacteria, thereby increasing bacterial acid resistance [33,34].

Wheat is a globally predominant cultivated crop, contributing to 30% of the globe's total grain production and half of the world's grain trade [35]. The wheat variety HD3086 (Pusa Gautami) was developed for cultivation under irrigation and appropriate sowing conditions in Northern India [36]. It has high resistance to yellow rust and other diseases and has a high protein content.

Coating ZnO NPs onto HD3086 seeds resulted in a 7% and 3% increase in root length and shoot length, respectively, in [37]. The priming of copper oxide nanoparticles along with the PGPB *Bacillus subtilis* exhibited a synergetic effect on the germination rate and other physiological parameters of growth when compared to that of the control in [38]. The treatment of wheat seeds with mesoporous silica (MS) NPs displayed a significant increase of 13.7% and 15.5% in seed germination with exposure to 500 and 2000 mg L^{-1} MS NPs, respectively, in [39].

Black wheat (NABI MG11) is a variety of wheat that has a dark-colored bran layer, giving it a black or dark purple appearance. The color is attributed to anthocyanins, which are known for their antioxidant properties and have been associated with various health benefits, including a reduced risk of chronic diseases such as heart disease and certain types of cancer [40]. The anthocyanin content of black wheat ranges from 100 to 200 ppm, whereas normal wheat typically contains 5 ppm. Furthermore, the protein content of black wheat was found to be 17% higher than that of the control wheat in [41]. Additionally, it has a higher level of essential fatty acids like linoleic and linolenic acids, ranging from 30% to 50% higher than that of regular wheat [42,43]. Along with possessing exceptional nutritional qualities, black wheat grain is a good source of micronutrients; it has more zinc, iron, copper, magnesium, and potassium than regular wheat [44]. Beyond this variety's potential health benefits, black wheat flour finds applications in culinary endeavors, serving as a key ingredient for crafting bread, pasta, and various baked goods. Its distinctive dark color not only contributes to its visual appeal but also adds an intriguing and aesthetic dimension to dishes. Black wheat is not as widely cultivated or readily available as conventional wheat varieties due to its comparatively low crop yield [40].

We investigated the potential of nanobiofertilizers synthesized using PGPB (*Bacillus* sp.) in combination with mesoporous silica (MS NPs), zinc oxide nanoparticles (ZnO NPs), and copper oxide nanoparticles (CuO NPs) in a study conducted using two varieties

of wheat (*Triticum aestivum*), NABI MG11 (black wheat) and HD3086 (brown wheat). Understanding the intricate interplay between bacteria and nanoparticles during priming is crucial for applications ranging from nanomedicine to environmental remediation. We explored the mechanisms, consequences, and potential applications of priming via bacteria–nanoparticle interactions for the generation of nanobiofertilizers, which contribute to sustainable development.

2. Materials and Methods

2.1. Traits of PGPB Isolates

The plant growth-promoting traits, such as IAA production, phosphate solubilization, and siderophore production, of the bacterial isolates CP4 and AHP3 have been reported earlier by Yadav et al. [12]. These two isolates alone and as part of consortia with arbuscular mycorrhizal fungi have been shown to enhance plant growth, yield, and nutrient uptake in wheat. Additional attributes that may contribute indirectly to plant growth promotion are given below:

Bacterial isolates were analyzed to determine their ability to produce ammonia by growing cultures for 48–72 h at 28 ± 2 °C in 10 mL of peptone water. A total of 0.5 mL of Nessler's reagent was added to each flask. Transition to a brown or yellow color signified ammonia production [45].

The isolates' ability to produce hydrogen cyanide (HCN) was tested using the Lorck (1948) method. Briefly, isolates were streaked on modified nutrient agar plates with glycine (4.4 g L^{-1}). The plate was covered with a filter paper socket filled with picric acid solution (2.5 g of picric acid and 12.5 g of sodium carbonate in 1 L of distilled H_2O). The plates were parafilm-sealed and incubated for 4 days at 28 ± 2 °C. HCN production was indicated by the orange-to-red color transition [46].

The catalase test was performed by placing a bacterial colony on a microscopic slide inside a Petri plate. A drop of 3% H_2O_2 was added to the colony. To prevent aerosols and to induce rapid bubbling, the Petri dish was covered with a lid [47].

2.2. Preparation of Nanoparticles

For nanoencapsulation, three nanoparticles were used. They were synthesized as follows:

2.2.1. Mesoporous Silica Nanoparticles

Stober's method was used to synthesize silicon dioxide nanoparticles, where 1.5 mL of tetraethyl orthosilicate (TEOS), 1 mL of deionized water, 1.7 mL of ammonia, and 50 mL of a solvent were incorporated into the reactive media. The reaction was then continued for a further 2 h under the same conditions after supplying an extra 1 mL of TEOS. The mixture was incubated at a temperature of 40 °C for 3 h in a magnetic stirrer and subsequently rinsed multiple times with deionized water; the residual solvents were eliminated using a rotary evaporator [48].

2.2.2. Zinc Oxide Nanoparticles

Small amounts of 2 M NaOH solution were added to 50 mL of 0.02 M zinc acetate solution until the pH reached 12 and then continuously stirred for 2 h. The white-colored synthesized precipitate was then washed multiple times with distilled water and placed in a hot air oven at 60 °C overnight [49].

2.2.3. Copper Oxide Nanoparticles

Copper chloride ($CuCl_2$) was dissolved in 100 mL distilled water to a concentration of 0.1 M. Next, 0.1 M sodium hydroxide solution was added, and the mixture stirred until the pH reached 14. The black precipitate obtained was rinsed with water and ethanol many times until the pH reached 7. The precipitate was dried at 80 °C for 16 h [50]. All three nanoparticles described above were characterized by scanning electron microscopy

(SEM) at the Central Instrumentation Laboratory (CIL), Central University of Punjab (CUPB), India.

2.3. Nanoencapsulation of PGPB Isolates

2.3.1. Physical Adherence of Bacteria to the NPs

Depending upon the surface charge of the nanoparticles and that of the bacterial isolates, physical adherence between isolates and nanoparticles was observed while they were suspended in phosphate-buffered saline (PBS). Both the bacterial isolates were grown in nutrient broth for 48 h until the cell density was 10^8 CFU mL^{-1}. The culture was then centrifuged twice at 5000× *g* for 10 min. The pellet was suspended in PBS at a concentration of 1 mg mL^{-1} nanoparticles and incubated for 3 h. This step was performed to facilitate the adherence of nanoparticles onto the bacterial cell wall and the internalization of some nanoparticles inside the bacterial cells.

2.3.2. SEM Investigation of the Nanobiofertilizers

The morphology of the synthesized nanobiofertilizers was analyzed using field emission scanning electron microscopy (FE-SEM), and their size was determined using ImageJ software version 1.54d. The nanobiofertilizer produced by the addition of nanoparticles in PBS to the bacterial pellet was incubated for 24 h. The resultant samples were then lyophilized and submitted to the CIL, CUPB, India, for FE-SEM analysis.

2.3.3. Viability of Nanoencapsulation

To check the viability of the bacteria after nanoencapsulation, the lyophilized nanobiofertilizer powder was inoculated into the nutrient broth and incubated at 37 °C for 24 h for revival. Then, they were streaked onto a nutrient agar plate to ascertain their viability.

2.4. Crop Establishment and Treatment Application

Two wheat (*T. aestivum*) cultivars, HD3086, and black wheat NABI MG11, were used to analyze the impact of various bionanofertilizers. The plants were grown in pots with 7-inch diameters containing 3 kg of native soil after sieving to remove any debris. In the first set, wheat seeds were subjected to three biofertilizer treatments with the two *Bacilli* species, AHP3 and CP4, individually and a combination of AHP3 and CP4. In the second set, wheat seeds were subjected to nine nanobiofertilizer treatments with three types of nanoparticles, mesoporous silica (MS) NPs, zinc oxide (ZnO) NPs, and copper oxide (CuO) NPs, combined with AHP3 and CP4. Moreover, three treatments involving only nanoparticles were given, in addition to a control treatment ©, wherein no treatment was given to the plants. Each treatment had three replicates, and each pot had three seedlings. The plants were grown in an open greenhouse.

Seed bacterization was carried out using surface-sterilized seeds. Briefly, the seeds were washed with 70% ethanol for 1 min and 0.5% sodium hypochlorite for 2 min, followed by multiple washes with distilled water. The PGPB isolates were cultured in LB broth at 37 °C until they reached a cell density of 10^8 CFU mL^{-1} and were harvested and centrifuged. The bacterial pellet was resuspended and diluted with PBS with nanoparticles suspended in PBS. The seeds were primed in the respective culture mixture and incubated for 3 h. Five seeds were sown in each pot at a depth of 1.5–2 cm into the soil and thinned to 3 seedlings per pot after 7 days of germination. The plants received a foliar application of the same inoculum suspension of nanobiofertilizers at a concentration of 1 mg 10 mL^{-1} of nanoparticles after 22 days of growth. The solution was sprayed uniformly until the whole phyllosphere of the plant was wet [51]. All other agronomic practices, such as irrigation and weeding, were kept the same for all the treatments [52].

2.5. Observed Responses and Measurement Methods

2.5.1. Agronomic and Physiological Traits

The morphological parameters of the plants, including root and shoot length and fresh weight, were analyzed after the 45-day pot culture experiment. After being gently uprooted from the soil, the plants were washed thrice with distilled water to eliminate the soil adhered to their surfaces. The fresh weights of the plants were recorded post blotting. Shoot and root lengths were measured with the aid of a metric scale [53].

Leaf chlorophyll content was measured by grinding 100 mg of finely cut fresh leaves in 2 mL of 80% acetone and incubating them overnight at 4 °C, followed by centrifugation at 10,000× *g* for 5 min. The supernatant was used to record absorbance at 645 nm and 663 nm using the acetone solvent as a blank. Total chlorophyll was calculated according to the following formula:

mg total chlorophyll/g = 20.2(A645) + 8.02 (A663) × V/1000 × W, where A = absorbance at a specific wavelength, V = final volume of chlorophyll extract in 80% acetone, and W = fresh weight of plant tissue extracted [54].

Subsequently, 100 mg of fresh leaves were ground in liquid nitrogen using a mortar and pestle, followed by the addition of chilled extraction buffer containing Tris-HCl of 50 mM (pH 7.5), EDTA (2 mM), and 2-mercaptoethanol (0.04% *v*/*v*), maintaining a 5:1 buffer-to-sample ratio. The sample was centrifuged at room temperature for 10 min at 12,000× *g*. Next, 100 µL of the supernatant was used to estimate the protein contents using a dye-binding method involving the use of the Coomassie Brilliant Blue dye, which binds to a protein, causing a shift in the absorption maximum of the dye from 465 to 595 nm and an increase in absorbance at 595 nm [55,56]. Total protein content was determined using a standard curve of bovine serum albumin (BSA) and expressed in percentage [57].

Proline content was estimated starting with the homogenization of 100 mg leaves using 3% sulphosalicylic acid in a mortar and pestle and centrifugation at 10,000× *g* for 20 min at 4 °C. Then, 1 mL of the supernatant was mixed with 0.5 mL each of acid ninhydrin and glacial acetic acid. The mixture was heated at 100 °C for 60 min with rapid cooling. Proline was extracted by the addition of 4 mL toluene. The absorbance of the upper layer was measured at 520 nm [58]. The standard curve of L-proline was used to determine the total proline content in mmol g^{-1} FW.

2.5.2. Nutrient Uptake

Leaf samples with a dry weight of 100 mg were digested by adding 2 mL of conc. H_2SO_4 and gentle heating until partially dissolved. After each sample was cooled, 30% H_2O_2 was added, and the sample was then heated again until the solution turned colorless and a volume of 100 mL was achieved. Nitrogen content was analyzed by adding 2 mL NaOH (2.5N) and 1 mL sodium silicate solution (10%) to 10 mL of digested material. To a 5 mL aliquot, Nessler's reagent was added. The development of a yellow color and absorbance at 525 nm indicated the presence of nitrogen. Total nitrogen content was estimated using the standard curve based on ammonium sulfate [$(NH_4)_2SO_4$] [59].

Phosphorous content was analyzed by adding 2.5 mL of 2.5N NaOH and 2 mL of molybdate reagent to 10 mL of the pre-digested sample. After making up the volume to 50 mL, 2 to 4 drops of stannous chloride solution were added, followed by a reading at 660 nm [60].

The elemental analysis of macro- and micronutrients such as magnesium, calcium, manganese, copper, iron, zinc, and selenium was performed by inductively coupled plasma mass spectrometry (ICP-MS) using the method described by Dogra et al. (2019) [61]. Briefly, 100 mg of wheat leaves were acid-digested with 7 mL of the digestion solution with 5 mL of 70% HNO_3 and 2 mL of H_2O_2 in the microwave at 120 °C for 1.2 h. The digested sample was filtered through a 0.4 µm syringe filter and diluted 10-fold with milli-Q water. The standard used was VHG-SM68-1-100, with standards 1, 2, 3, and 4 set at 0.929, 4.92, 9.827, and 25.852 parts per billion (ppb), respectively. The samples were analyzed using ICP-MS by the CIL of the CUPB, India.

2.5.3. Soil Chemical Properties

The properties of the soil, such as soil organic carbon (SOC), were measured following the standard methods. To 0.5–1 g of dry soil, 10 mL $K_2Cr_2O_7$ (1N) and 20 mL concentrated H_2SO_4 were added and allowed to stand for 30 min. Subsequently, 200 mL distilled water, 10 mL phosphoric acid, and 1 mL diphenylamine solution were added. The resulting solution was titrated against ferrous sulphate solution until the solution reached its endpoint, which was the appearance of a brilliant green color [62]. The % of total organic carbon in the soil was calculated as per Walkley (1947) [63].

2.5.4. Soil Enzyme Activity

To measure invertase activity, 3 g of dry soil was taken in an Erlenmeyer flask, and 0.2 mL toluene, 5 mL modified universal buffer [64], and 5 mL sucrose solution (10%) were added. The mixture was incubated at 37 °C for 24 h, followed by filtration using the Whatman filter paper (no. 42). Then, 5 mL distilled water was added to one mL aliquot, followed by the addition of 2 mL NaOH (2 M) and 2 mL of the reagent prepared using 2,3-dinitro salicylic acid. The sample was incubated in a boiling water bath for 5 min and cooled to room temperature. The intensity of the color developed was measured at 540 nm. A graph was plotted to ascertain the obtained reducing sugar content with glucose/fructose (1:1) standard solution [65].

To measure dehydrogenase activity, 5 g samples of dried and finely powdered soil were taken, and 3% 2,3,5-triphenyl tetrazolium chloride (1 mL) and water (2.5 mL) were added. The samples were incubated for 24 h at 37 °C, followed by the extraction of the product triphenyl-formazan (TPF) using 10 mL of methanol. Absorbance was recorded at 485 nm. The activity of the enzyme was expressed as μg TPF g^{-1} soil 24 h^{-1} [66].

2.6. Statistical and Correlation Analyses

Statistical analysis for plant growth trait-related parameters and other attributes and soil physiochemical analysis were carried out by conducting a one-way ANOVA (analysis of variance) and Tukey's multiple comparisons tests (GraphPad Prism™ software version 8.0.1) for each treatment with the control, treatments of nanoparticles and bacteria with bacterial isolates as controls, and treatments of nanoparticles and bacteria with nanoparticles as controls. The results are represented as mean ± SD. All the parameters were tested in triplicate.

3. Results

3.1. Plant Growth-Promoting Attributes of CP4 and AHP3

The bacterial isolates CP4 and AHP3, belonging to *Bacillus* sp., were previously shown to produce IAA and siderophores and solubilize phosphate [12]. The ammonia test showed positive results for both isolates, which shows their ability to fix atmospheric nitrogen, which can be utilized by the host plants as a nitrogen source [67]. Hydrogen cyanide (HCN) is a secondary metabolite produced by bacterial cyanogenesis that can provide biocontrol for plants against living organisms like plant pathogens and predators [68]. The qualitative test performed for the detection of HCN production turned out to be positive in both bacterial isolates. The results indicate that CP4 and AHP3 act as natural protectors against plant pathogens contributing to plant growth promotion indirectly. Catalase production, a common trait of PGPB, protects plants from oxidative damage induced by reactive oxygen species (ROS), thereby maintaining redox balance in the plant cell [69]. Both the *Bacillus* strains showed positive results for the catalase test, as indicated by the formation of bubbles, with intense bubble formation by CP4 being observed.

3.2. SEM Analysis of Nanoparticles and Nanobiofertilizers

The morphological structures of the three types of nanoparticles, copper oxide NPs, mesoporous silica NPs, and zinc oxide NPs, are depicted in Figure 1a, Figure 1c, and Figure 1e, respectively. CuO NPs are seen as flower-shaped structures and have a size

ranging from 50 to 120 nm, with a mean diameter of 101 nm. MS NPs are spherical in shape, have pores on their surface, range in size from 50 to 130 nm, and have an average diameter of 94 nm, and ZnO NPs are seen as clustered, spherical, and amorphous structures and have sizes ranging from 70 to 180 nm, with an average diameter of 118 nm. The average size of the bacteria is 1.53 µm in length and 0.65 µm in breadth. The three nanobiofertilizers synthesized with the above-mentioned three types of NPs are shown in Figure 1b,d,f. Some nanoparticles containing positive charges are adsorbed onto the surface of the rod-shaped *Bacillus* species bacteria mostly due to the surface charge attraction between bacteria and nanoparticles (Figure 1), while some might be internalized. Therefore, the proportion of nanoparticles interacting with each bacterial cell is not known. The SEM micrograph shows a uniform distribution of nanoparticles over the bacterial cell wall. It is likely that the nanoparticles that were internalized in the bacterial cells might have interacted positively with the vital genes responsible for plant growth hormone production and other attributes, leading to plant growth promotion in wheat. As the experiments were carried out using fresh cultures of bacteria, no spore formation was seen, but as the bacteria used were spore-forming bacteria, there is the utmost possibility that upon storage for a longer duration, spore formation could have occurred. The final product/nanobiofertilizer in nutrient broth was 10^8 CFU mL^{-1}.

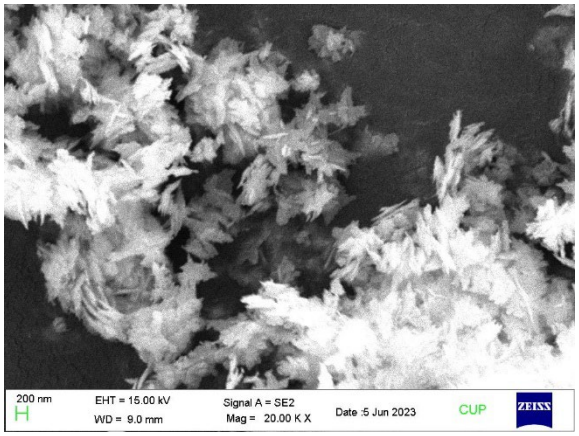

(**a**)

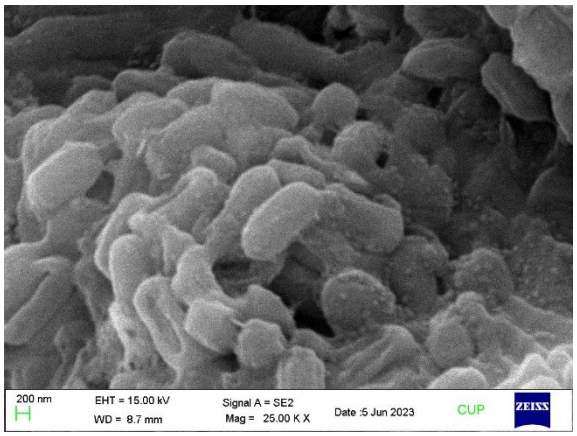

(**b**)

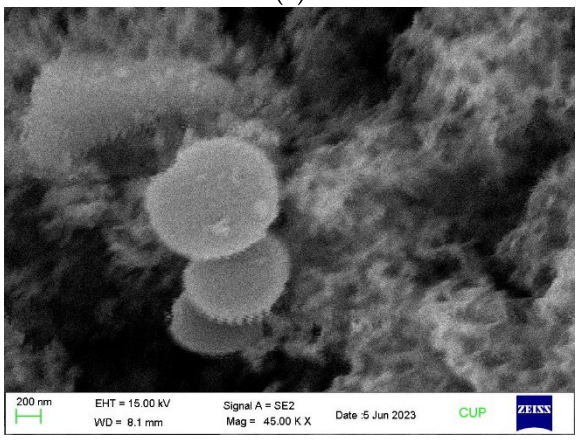

(**c**)

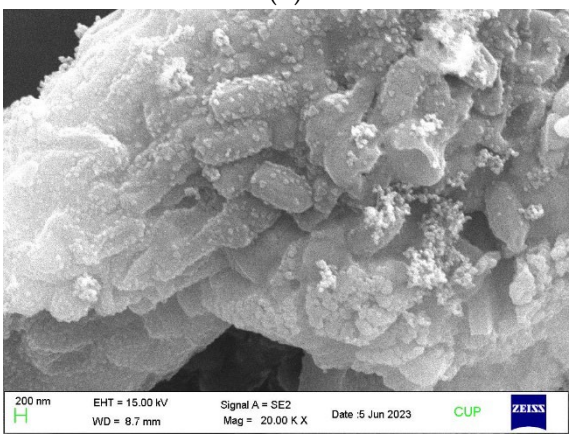

(**d**)

Figure 1. *Cont.*

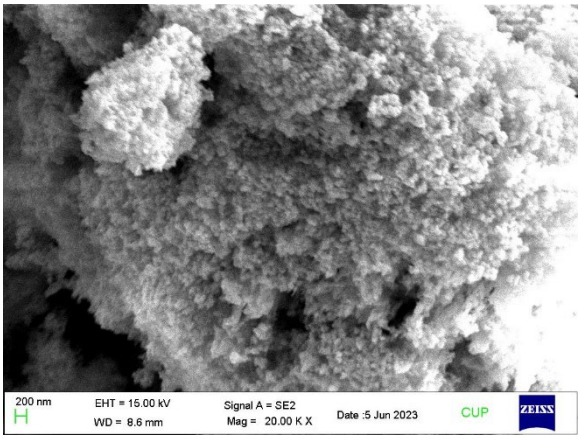

(**e**)

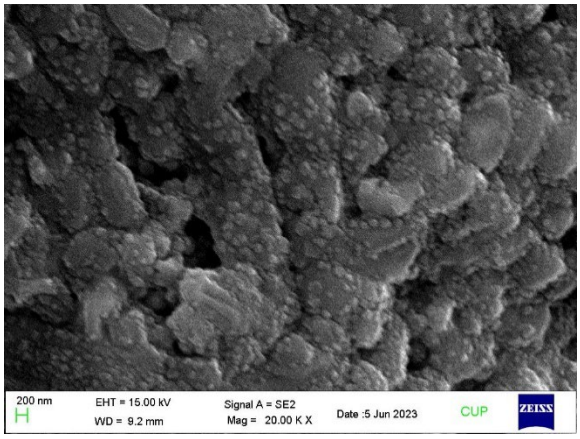

(**f**)

Figure 1. SEM micrograph of synthesized nanoparticles and nanobiofertilizers. (**a**) CuO NPs, (**b**) CuO NPs + CP4 + AHP3, (**c**) MS NPs, (**d**) MS NPs + CP4 + AHP3, (**e**) ZnO NPs, and (**f**) ZnO NPs + CP4 + AHP3.

3.3. Differential Effects of Biofertilizers, Nanofertilizers, and Nanobiofertilizers on Plant Growth Attributes and Biochemical and Physiological Parameters

3.3.1. Shoot and Root Length

In black wheat, a significant increase in shoot and root length was recorded for the treatments with MS NPs combined with PGPB, with the highest value being recorded for the CP4 + MS treatment, which achieved an increase of 110.7% and 134% in shoot and root length, respectively, when compared with the shoot and root length values of the control treatment (Figure 2a). When AHP3 was taken as a control, both the AHP3 + MS and AHP3 + ZnO treatments showed a significant increase of 72.6% in shoot length and 73.7% in root length and 48.4% in shoot length and 86% in root length, respectively, but significant increases were not found for the AHP3 + CuO treatment. Among the CuO NP treatments, a significant increase in root length could be observed only when compared with the control. AHP3 and CP4 alone and in conjunction with ZnO showed a significant increase in the root length of black wheat. These results are in accordance with previous findings showing that Zn nanoparticles and mesoporous silica nanoparticles are plant shoot and root growth promoters, while AHP3 and CP4 have shown plant growth promotion in previous studies [12,52,70–72]. Furthermore, CuO NPs, AHP3 + CuO NPs, and CP4 + CuO NPs did not show any significant increase in plant shoot and root lengths compared to the control. This also resonates with the previous findings that copper being present in excess inhibits the plant's normal growth by interfering with plant nutrient absorption, photosynthesis, root development, and leaf extension, and affects the functions of some key cellular components, such as proteins, lipids, DNA, and RNA [73,74].

In the HD3086 variety, the treatments with ZnO NPs and CP4 alone showed the highest significant increase in both shoot and root length when compared with the control (Figure 2b). Root length was observed to be the highest in the CP4 treatment, with a value of 31.3 cm and a percentage increase of 49.52%. Meanwhile, the highest shoot length was recorded for CP4 + ZnO, with a value of 23.7 cm and a 66.5% increase when compared with that of the control. CP4 + AHP3 together as a consortium with and without nanoparticles did not show any increase in the root and shoot lengths of the plants compared to their respective controls. In our previous study [71], CP4 was characterized to be Bacillus subtilis, and it is known to release numerous genetically encoded molecules that regulate the growth of neighboring organisms [75]. AHP3 and CP4, as controls and in combination with their respective NP treatments, showed a significant increase with the MS and ZnO NPs treatment sets.

AHP3 and CP4 alone and in combination with MS NPs as part of a consortium in black wheat, as well as AHP3 alone with MS NPs in HD3086, showed a significant increase

in shoot length when the MS treatment was taken as a control. When the ZnO treatment was taken as a control, CP4 alone with ZnO showed a significant increase in shoot length in HD3086. When the MS NPs treatment was taken as a control, only CP4 with MS NPs in black wheat and AHP3 with MS NPs in HD3086 showed a significant increase in root length. When CuO was taken as a control, AHP3 and CP4 alone with CuO NPs showed a significant increase in the root length of black wheat. When the CuO treatment was taken as a control, only AHP3 and CP4 in conjunction with CuO showed a significant increase in shoot length.

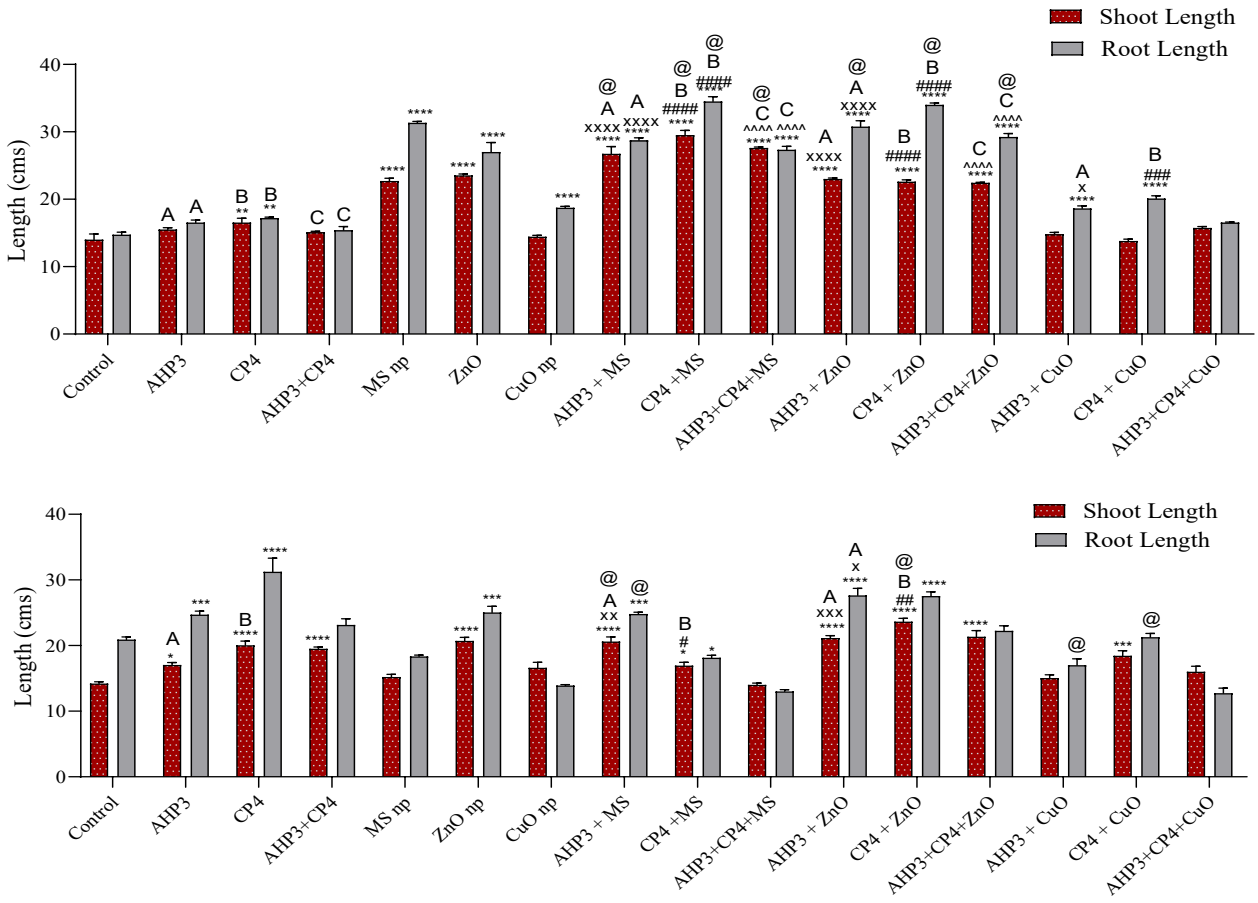

Figure 2. Shoot and root lengths of black wheat and HD3086 with different combinations of PGPB and nanoparticles. (**a**) Black wheat and (**b**) wheat variety HD3086. Values are shown as mean ± standard error. A, B, and C denote the AHP3, CP4, and AHP3 + CP4 treatments, respectively, and the symbols '*', 'x', '#', and '^' depict statistically significant values ($p < 0.05$) compared to the control, AHP3, CP4, and AHP3 + CP4 treatments as controls, respectively (based on our ANOVA). Highly significant values are depicted by the same symbols 2, 3 and 4 times at $p < 0.01$, $p < 0.001$, $p < 0.0001$, respectively. The symbol '@' denotes the statistically significant values of NBFs compared to their respective nanoparticle-only treatments (based on our ANOVA).

3.3.2. Plant Fresh Weight

The highest plant fresh weight value was found for black wheat plants treated with the AHP3 + CP4 + MS NPs (8.6 g) (Figure 3a). The black wheat fresh weight values showed a significant increase in all the MS NP sets compared to the control plants. However, AHP3, CP4, and AHP3 + CP4 singly and in combination with CuO NPs did not cause any increase in the fresh weight values of the plants when compared with the control. While considering AHP3 as a control, only AHP3 + MS showed a highly significant increase of 62.7%. A similar result was also seen for CP4 + MS while comparing with CP4 as a control, with an increase of 136.5%. Likewise, the consortia treatment (AHP3 + CP4) with MS,

when compared with consortia as a control, showed an increase of 214.7%. When the MS treatment was taken as a control, AHP3 and CP4 alone and in conjunction with MS showed a significant increase in black wheat fresh weight. When CuO was taken as a control, AHP3 and CP4 in conjunction with CuO showed a significant increase in the fresh weight values of the black wheat plants.

In the HD3086 plants, when compared with the control, only the CuO and ZnO NPs alone and ZnO NPs in combination with PGPB showed a highly significant increase in plant fresh weight values (Figure 3b). When taking AHP3 as a control, only the AHP3 + ZnO treatment showed a significant increase (14.28%). A similar result was observed when taking CP4 and AHP3 + CP4 as controls, with an increase of 150% (CP4 + ZnO) and 119% (AHP3 + CP4 + ZnO), respectively. The results showed that PGPB and nanoparticles contribute to increasing the fresh weights of plants, as per previous reports [76,77], and among the types of three nanoparticles, i.e., Zn, Si, and Cu, the zinc NPs were found to be the most effective in increasing the fresh weight values of the plants.

(**a**)

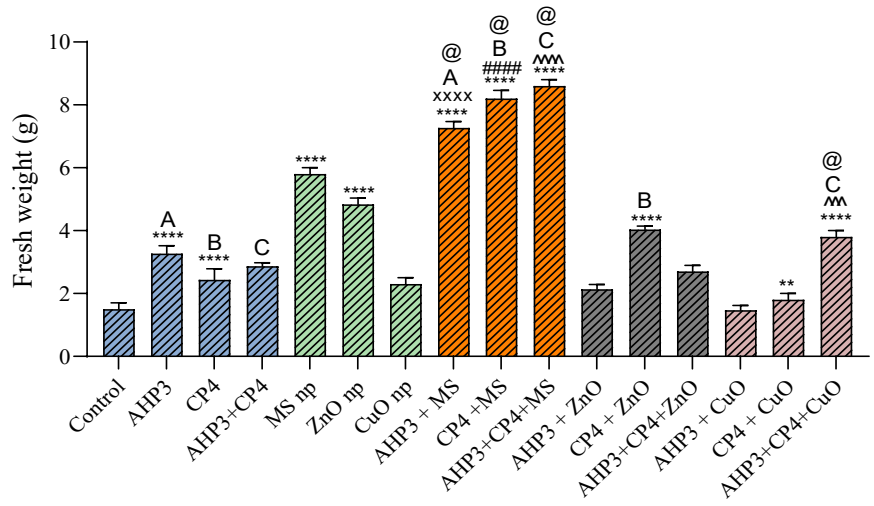

(**b**)

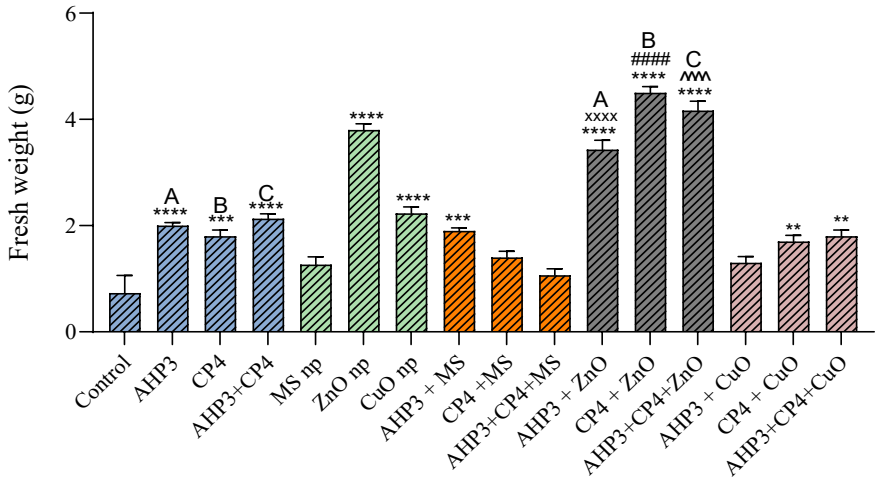

Figure 3. Fresh weights of black wheat and HD3086 plants with different combinations of PGPB and nanoparticles. (**a**) Black wheat and (**b**) wheat variety HD3086. Annotations and statistical significance are as described in Figure 2.

3.3.3. Photosynthetic Pigments

When compared with the control treatment, a highly significant increase in total chlorophyll was observed in the black wheat plants treated with a consortia of AHP3 and CP4, AHP3 + CP4 + ZnO, ZnO and MS NPs, and AHP3 + MS (Figure 4a). Also,

among all the treatment sets, a maximum increase of 68.7% and value of 1.95 mg g^{-1} FW were recorded in AHP3 + CP4 + ZnO-inoculated black wheat, and an increase of 45.95% with a value of 1.69 mg g^{-1} FW were observed in plants inoculated with ZnO NP. When ZnO was taken as a control, AHP3 and CP4 in conjunction with ZnO was found to induce a significant increase in the chlorophyll contents of the black wheat plants. Our findings showed that among the three types of nanoparticles, zinc, copper, and mesoporous silica nanoparticles, the zinc nanoparticles were found to be most effective in increasing the chlorophyll content, and this effect was enhanced when they were supplemented with PGPB.

When compared with the control, the wheat variety HD3086 showed a much more significant increase in the total chlorophyll values of plants treated with ZnO NPs in combination with PGPB (Figure 4b). When AHP3 and CP4 were considered as controls and compared with their respective NP treatments, only AHP3 + ZnO and CP4 + ZnO showed a highly significant elevation, with values of 1.3 mg g^{-1} FW and 1.46 mg/g FW. Notably, the consortia treatment within the MS NP set also exhibited an elevated chlorophyll content with a value of 1.33 mg g^{-1} FW. When the MS NP treatment was taken as a control, AHP3 and CP4 in conjunction with MS were observed to induce a significant increase in chlorophyll in the HD3086 plants.

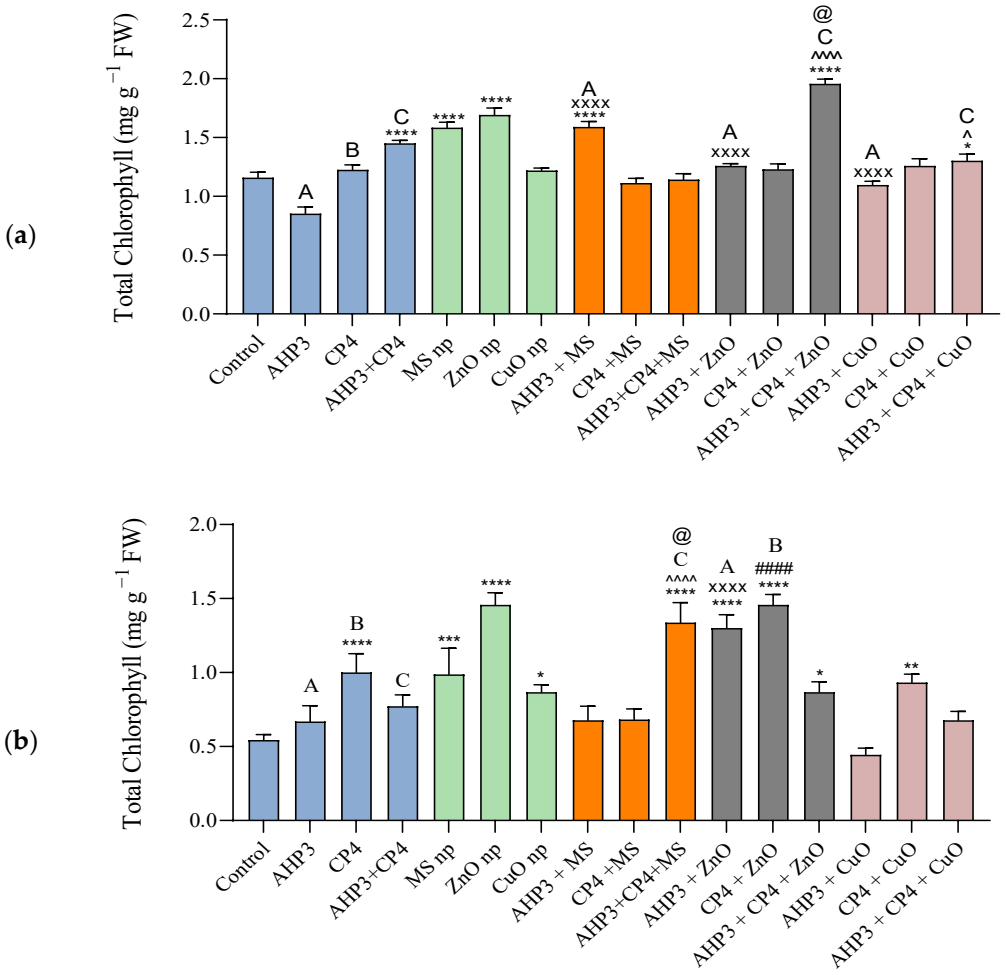

Figure 4. Total chlorophyll content of leaves of black wheat and HD3086 plants with different combinations of PGPB and nanoparticles. (**a**) Black wheat and (**b**) wheat variety HD3086. Annotations and statistical significance are as described in Figure 2.

3.3.4. Total Soluble Protein Content

In black wheat, the CuO NP treatment expressed the highest total soluble protein value among the three types of nanoparticle treatments. When the nanoparticles were combined with PGPB, all the sets showed better results than the control experimental setup. For the treatment with ZnO NPs, the AHP3 and CP4 combination showed the highest increase of 256%, with a value of 0.51 mg g^{-1} FW (Figure 5a). When AHP3 was considered as a control and compared with the other treatments involving AHP3 in tandem with NPs, AHP3 + ZnO exhibited the highest significance, with an increase of 75.3% and with a value of 0.4 mg g^{-1} FW, whereas the AHP3 with MS treatment showed an increase but only with a value of 0.24 mg g^{-1} FW. The AHP3 + CuO treatment also showed an increase of 65.2%. Likewise, when CP4 was considered as a control and compared with other treatments of CP4 with NPs, highly significant increases were found in the plants that received the CP4 + ZnO (185%) and CP4 + CuO (129.7%) treatments. When the MS NP treatment was taken as a control, AHP3 and CP4 in conjunction with MS showed a significant increase in the protein contents of the black wheat plants. When ZnO was taken as a control, AHP3 and CP4 in conjunction with ZnO showed a significant increase in the protein contents of the black wheat plants.

In the context of HD3086, all the treatments with ZnO showed a statistically significant increase in comparison with the control and other treatments with nanoparticles (Figure 5b). Among all these, the AHP3 + CP4 + ZnO treatment showed the highest value of 0.24 mg g^{-1} FW, representing a notable increase of 132.3%. When AHP3 and CP4 were considered as controls and compared with their respective NP treatments, all corresponding ZnO treatments with both AHP3 and CP4 demonstrated highly significant values. Specifically, when considering the consortia of AHP3 + CP4 as a control, only AHP3 + CP4 in conjunction with ZnO NP exhibited a noteworthy increase (71.4%). These findings underscore the specific efficacy of ZnO treatments, particularly the synergistic effect observed with AHP3 and CP4 combinations. The substantial enhancement in total soluble protein content suggests the potential utility of these treatments in modulating biochemical processes in brown wheat HD3086, warranting further exploration for agricultural applications.

(**a**)

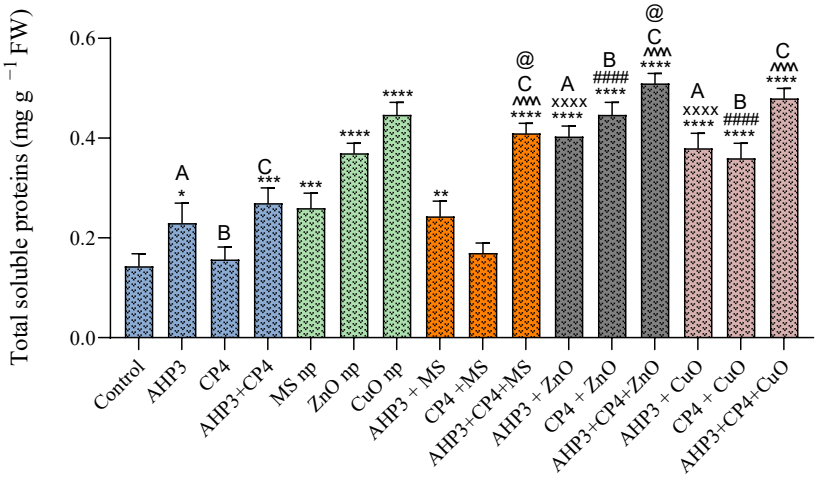

Figure 5. *Cont.*

(**b**)

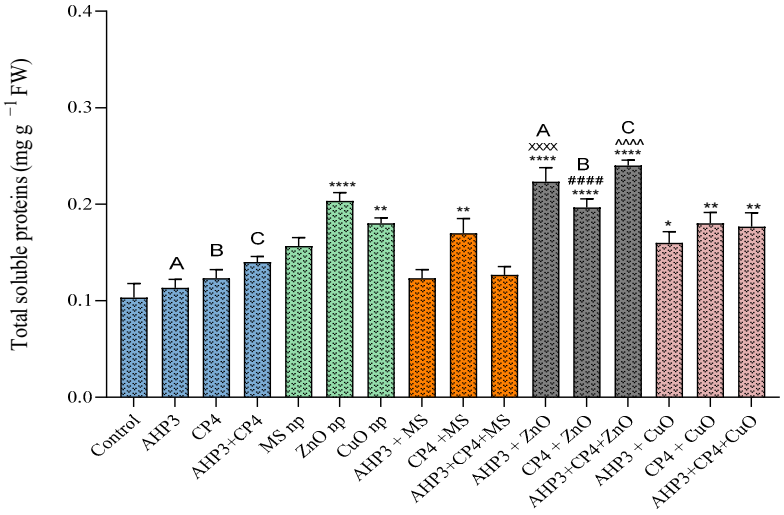

Figure 5. Total protein contents of leaves of black wheat and HD3086 plants with different combinations of PGPB and nanoparticles. (**a**) Black wheat and (**b**) wheat variety HD3086. Annotations and statistical significance are as described in Figure 2.

3.3.5. Proline Content

In both the black wheat and HD3086 wheat cultivars, the highest proline content was observed in plants subjected to the MS NP treatment and its combination with PGPB. In black wheat, the application of MS NPs resulted in the most substantial increase of 190%, with a recorded value of 12.65 µmoles g^{-1} FW, compared to the control (Figure 6a). Also, all the treatments indicated a significant rise in proline content, except for the AHP3 + ZnO treatment and sole ZnO NP application treatment. When AHP3 was considered as a control and compared with the other treatments involving AHP3 in tandem with NP, AHP3 + MS exhibited the highest significance, with an increase of 117% and a value of 12.4 µmoles g^{-1} FW. The AHP3 + CuO treatment also exhibited a notable increase of 51.3%. Similarly, when CP4 was considered as a control and compared with the other treatments involving CP4 in tandem with NP, highly significant increases were observed in plants treated with the CP4 + CuO (35.7%) and CP4 +MS (18%).

In HD3086, all the treatments except MS NP, Cuo NP, and AHP3 + ZnO showed a statistically significant increase in comparison with the control (Figure 6b). Among all the treatments, the AHP3 + MS treatment showed the highest value of 8.27 µmoles g^{-1} FW and a 266% increase ($p < 0.0001$). When AHP3 and CP4 were considered as controls and compared with their respective NP treatments, only the treatments with MS NPs were found to exert a highly significant effect. The consortia (AHP3 + CP4), when taken as a control and compared with both the MS and ZnO NP treatments, showed highly significant increases of 36% and 119%, respectively.

When the MS treatment was taken as a control, AHP3 and CP4 alone and in conjunction with MS showed a significant increase in proline in HD3086. When ZnO was taken as a control, CP4 alone and in conjunction with AHP3 and ZnO showed a significant increase in proline in the black wheat plants, and AHP3 and CP4 in conjunction showed a significant increase in proline in the HD3086 plants. When CuO was taken as a control, CP4 alone with CuO in black wheat and AHP3 and CP4 alone with CuO in HD3086 showed a significant increase in proline. These findings underscore the effectiveness of MS NP treatments, either alone or in combination with PGPB, in inducing proline accumulation in both black wheat and HD3086 cultivars. The substantial increases in proline content suggest a potential role in stress response and tolerance mechanisms.

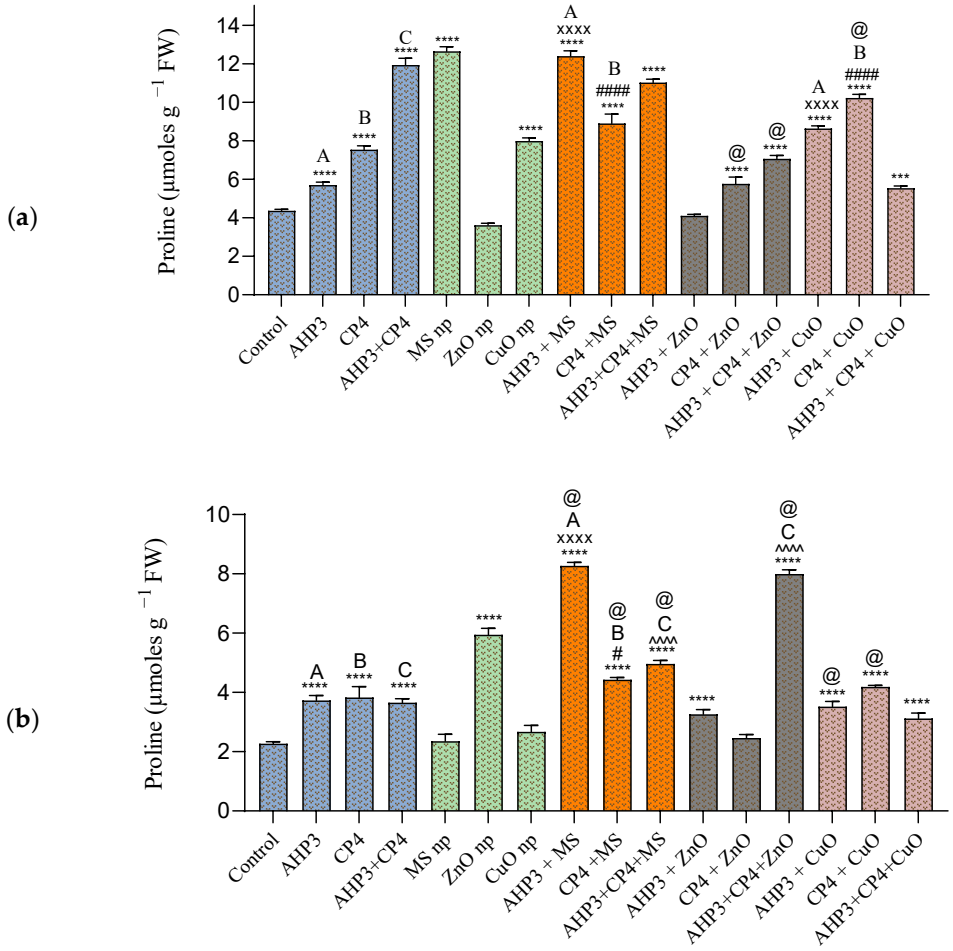

Figure 6. Total proline content in leaves of black wheat and HD3086 plants with different combinations of PGPB and nanoparticles. (**a**) Black wheat and (**b**) wheat variety HD3086. Annotations and statistical significance are as described in Figure 2.

3.3.6. Nitrogen Uptake

Nitrogen (N) in black wheat leaves (Figure 7a) showed a significant increase in all the treatments with ZnO and CuO NPs in combination with PGPB. The most substantial increase was found in AHP3 + ZnO, with a value of N of 3.92%, resulting from a remarkable increase of 353%. However, a significant increase was not observed in the MS NP combinations, except in the cases of MS and AHP3 + CP4 + MS. When AHP3 was used as a control, both AHP3 + ZnO and AHP3 + CuO demonstrated increases of 328.5% and 77%, respectively. Similarly, the treatments involving CP4 + ZnO and CP4 + CuO showed substantial increases compared to the use of CP4 alone. Notably, all the treatments involving consortia with NP surpassed the nitrogen content of the consortium alone. When CuO was taken as a control, AHP3 and CP4 in conjunction with CuO in black wheat showed a significant increase in nitrogen.

In HD3086, all the treatments exhibited significantly higher nitrogen values, except for CP4 and AHP3 + CP4, when compared to the control (Figure 7b). The AHP3 + MS showed the highest value of 3.86% of N. All the treatments involving NP with PGPB combinations showed a considerable rise in N compared to their respective controls. When MS treatment was taken as a control, AHP3 and CP4 alone with MS showed a significant increase in nitrogen in HD3086. When ZnO was taken as a control, AHP3 and CP4 in conjunction with ZnO showed a significant increase in nitrogen in HD3086. In the context of current data, these findings align with the existing knowledge on the positive impact of nanoparticles and PGPB on nutrient content in plants. The substantial increases in nitrogen, particularly in the AHP3 + ZnO treatment in black wheat and AHP3 + MS treatment in HD3086, suggest

the potential of these treatments in enhancing nutrient uptake and assimilation. The results underscore the importance of considering specific treatments for different wheat varieties, reflecting the complex interactions among nanoparticles, PGPB, and plant responses.

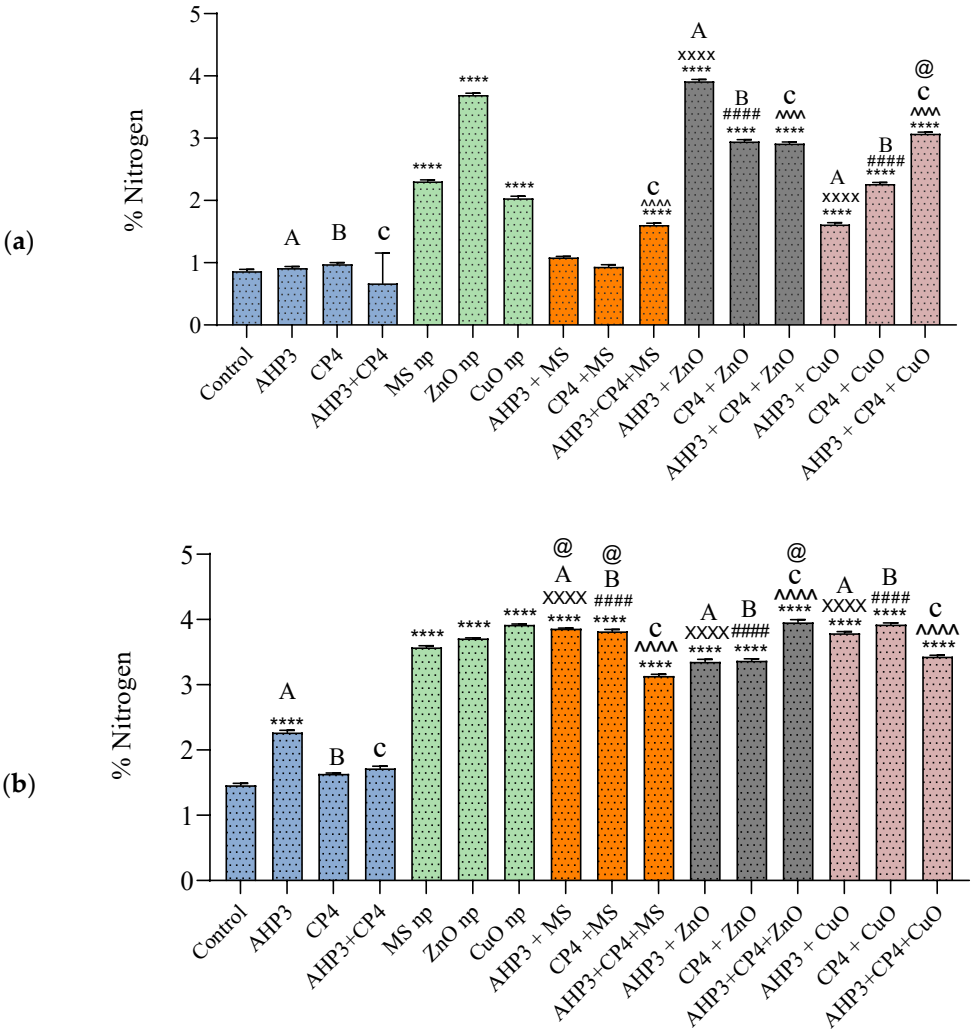

Figure 7. Nitrogen in leaves of black wheat and HD3086 plants with different combinations of PGPB and nanoparticles. (**a**) Black wheat and (**b**) wheat variety HD3086. Annotations and statistical significance are as described in Figure 2.

3.3.7. Phosphorus Uptake

In both sets of wheat cultivars, while comparing the phosphorus in only bacterial treatments, CP4 displayed the highest value. Notably, in black wheat, all the treatments recorded significant elevations when compared with the control, except for the AHP3 + CP4, MS NP, and ZnO NP treatments (Figure 8a). When AHP3 and its corresponding NP treatments were compared, all three NP combinations, AHP3 + ZnO, AHP3 + MS, and AHP3 + CuO, showed a significant increase, with phosphorus values of 0.77%, 0.81%, and 0.88%, respectively. Of these, the AHP3 + CuO combination recorded the best response, with a 60% increase when compared to AHP3 alone.

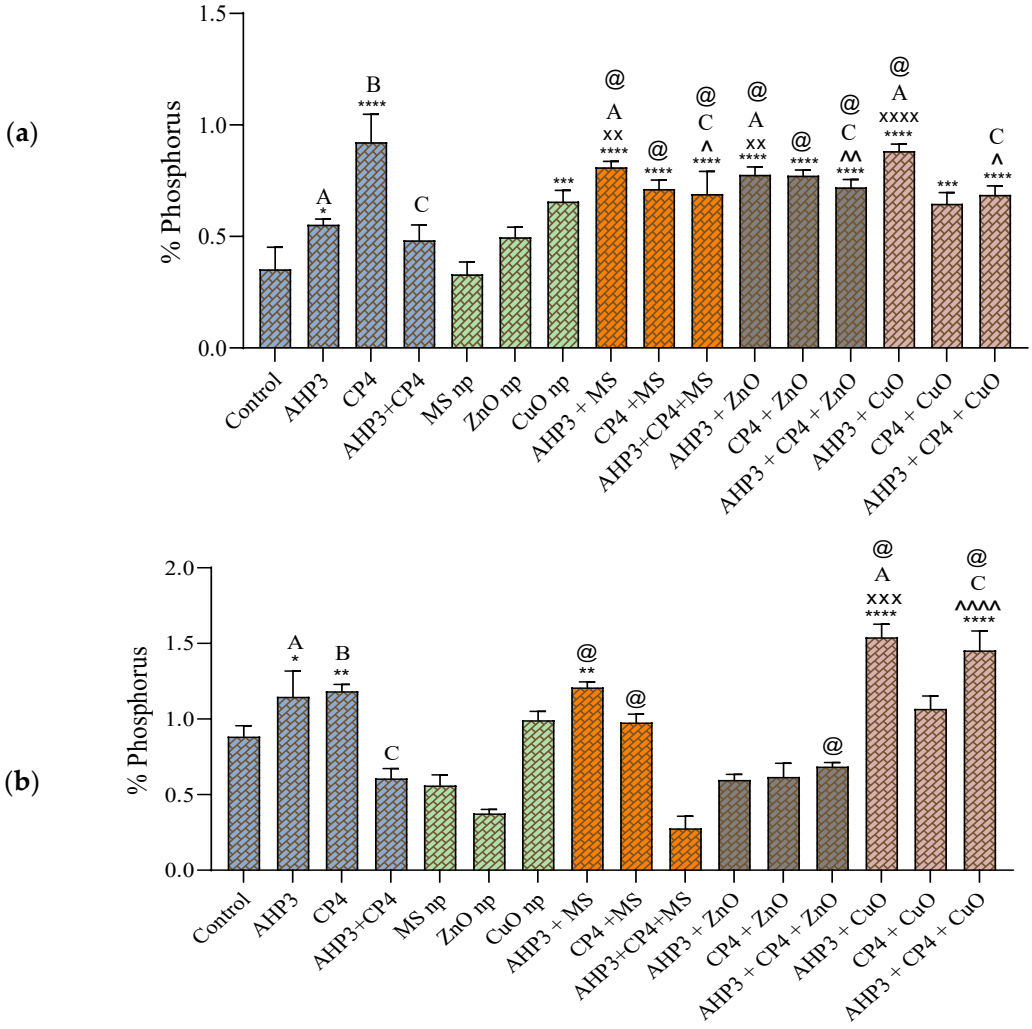

Figure 8. Phosphorus in leaves of black wheat and HD3086 plants with different combinations of PGPB and nanoparticles. (**a**) Black wheat and (**b**) wheat variety HD3086. Annotations and statistical significance are as described in Figure 2.

It is worth noting that none of the plants inoculated with CP4 along with NPs exhibited a significant increase when compared to the sole CP4 treatment, highlighting the unique role of CP4 in phosphorus enhancement (Figure 8a). Moreover, the phosphorus in the NP treatment of consortia in combination with each of the three types of NPs showed a significant increase when compared to the consortia treatment alone. Notably, AHP3 + CP4 + ZnO exhibited the highest percent increase of 50%, reaching 0.7% phosphorus in the leaves, underscoring the synergistic effects of the combined treatments.

In the HD3086 variety, various treatments, including AHP3, CP4, AHP3 + MS, AHP3 + CuO, and AHP3 + CP4 + CuO demonstrated a significant increase in phosphorus when compared to the control (Figure 8b). The highest value was recorded for AHP3 + CuO, with a phosphorus value of 1.4%, with a substantial 64.8% increase compared to the control and a 27.2% increase compared to AHP3 alone. However, the treatments with ZnO NPs and PGPB showed a significant decrease when compared to the control. When comparing the consortia treatment with its respective NP treatments, only AHP3 + CP4 + CuO showed a highly significant increase of 137.7%.

When the MS treatment was taken as a control, AHP3 and CP4 alone and in conjunction with MS in black wheat and AHP3 and CP4 alone with MS in HD3086 showed a significant increase in phosphorus. When ZnO was taken as a control, AHP3 and CP4 alone and in conjunction with ZnO in black wheat and AHP3 and CP4 in conjunction with ZnO in HD3086 showed a significant increase in phosphorus. When CuO was taken as a control, AHP3 alone with CuO in black wheat and AHP3 alone and in conjunction with CP4 and CuO in HD3086 showed a significant increase in phosphorus. These findings underscore the critical role of specific bacterial strains such as CP4 and tailored NP combinations in modulating phosphorus levels in wheat plants.

3.4. ICP-MS Analysis Identified Enhancement of Macro- and Micronutrients

In addition to the assessments of nitrogen and phosphorus, the estimation of macro- and micronutrients using ICP-MS revealed that various nanoparticles in conjunction with AHP3 induced substantial increases when compared to the control in the black wheat variety. Specifically, the highest amount of magnesium was observed in AHP3 + CP4 + CuO, with an increase of 429%. Notably, all the treatments showed a statistically significant increase in Mg when compared to the control (Table 1). The treatment involving CuO NPs showed the highest amount of calcium and manganese, with CuO NPs alone yielding the highest concentration of calcium and AHP3 + CuO showing the highest concentration of manganese. The application of CuO NPs increased the amount of copper in the leaves. Interestingly, this observation was not mirrored in plants treated with the ZnO NP treatment, where the highest amount of ZnO was observed in plants treated with PGPB alone. The highest amount of iron was observed in plants treated with AHP3 + CP4 + MS, exhibiting a notable increase of 31.7%, while the CP4 + ZnO treatment displayed the highest selenium value. These findings indicate the diverse and specific responses of nutrient uptake in black wheat under various nanoparticle treatments. The substantial increases in magnesium, calcium, manganese, copper, iron, zinc, and selenium levels underscore the potential of tailored nanoparticle applications in enhancing nutrient availability and uptake. These results contribute valuable insights into optimizing nutrient management practices for improved crop nutrition and overall plant health in agricultural systems. Further investigations into the underlying mechanisms of nanoparticle-induced nutrient changes could offer valuable information for sustainable and precision agriculture strategies.

In the wheat variety HD3086, noteworthy increases in the concentration of both macro- and micronutrients were observed in treatments involving CP4 + MS and AHP3 + ZnO compared to the control. Particularly, these treatments exhibited a significant increase in magnesium, with percentage increases of 237.6% and 268%, respectively (Table 2). The combined application of CuO NP and PGPB exhibited an increase in copper and zinc. The element selenium showed maximum levels in AHP3 + CuO and CP4 + ZnO treatment with impressive increases of 617.2% and 257%, respectively. The treatment of CP4 + MS demonstrated a remarkable surge in zinc, reaching a value of 2276.8 mg kg^{-1}. Moreover, an increase in manganese was evident in MS and ZnO treatments in combination with PGPB, with CP4 + MS showing the highest value with a percentage increase of 205% compared to the control. Overall, the concentrations of macro- and micronutrients exhibited a notable increase in treatments combining ZnO NP and PGPB compared to the control. These results highlight the effectiveness of using ZnO and MS NPs and combining them with PGPB to enhance nutrient uptake in HD3086 wheat. The observed increases in magnesium, copper, zinc, selenium, and manganese underscore the potential role of tailored nutrient management strategies in promoting plant health and nutrient utilization.

Table 1. Macro- and micronutrients in leaves of black wheat cultivar treated with different combinations of PGPB and nanoparticles.

	Mg [mg kg^{-1}]	Ca [mg kg^{-1}]	Mn [mg kg^{-1}]	Fe [mg kg^{-1}]	Cu [mg kg^{-1}]	Zn [mg kg^{-1}]	Se [mg kg^{-1}]
Control	1678 ± 0.8	112 ± 3	50 ± 1	506 ± 11	22 ± 0.5	131 ± 2	43 ± 2
AHP3	* 1786 ± 3	* 260 ± 5	81 ± 2	* 661 ± 22	10 ± 0.6	* 237 ± 5	∞ 64 ± 4
CP4	* 1940 ± 21	* 213 ± 3	92 ± 0.4	* 609 ± 9	22 ± 0.4	* 235 ± 6	**∞ 78 ± 4**
AHP3 + CP4	* 1978 ± 25	113 ± 3	91 ± 1	493 ± 22	5 ± 0.3	*** 540 ± 1**	46 ± 1
AHP3 + MS	* 2110 ± 9 x	* 188 ± 1	71 ± 0.3	* 643 ± 11	5 ± 0.2	* 219 ± 5	∞ 57 ± 3
CP4 + MS	* 2265 ± 45 #	165 ± 2	111 ± 2	531 ± 24	6 ± 0.1	---	52 ± 3
AHP3 + CP4 + MS	* 1795 ± 10 ^	* 235 ± 4 ^	64 ± 1	317 ± 11	19 ± 0.4	47 ± 1	∞ 60 ± 5
MS NP	* 2398 ± 13	146 ± 3	98 ± 1	*** 667 ± 12**	11 ± 0.2	* 518 ± 6	53 ± 1
AHP3 + ZnO	* 5106 ± 50 x	79 ± 2	94 ± 1	482 ± 29	17 ± 0.6	99 ± 2	48 ± 2
CP4 + ZnO	* 6132 ± 71 #	109 ± 6	96 ± 1	* 636 ± 8	19 ± 0.4	94 ± 5	∞ 63 ± 4
AHP3 + CP4 + ZnO	* 5756 ± 157 ^	115 ± 5	83 ± 1	5650 ± 10	13 ± 0.8	42 ± 4	52 ± 4
ZnO NP	* 5555 ± 67	79 ± 4	108 ± 2	557 ± 9	18 ± 0.2	53 ± 3	54 ± 1
AHP3 + CuO	* 7411 ± 84 x	81 ± 3	117 ± 1	* 599 ± 46	∞ 30 ± 0.4	126 ± 4	52 ± 3
CP4 + CuO	* 5333 ± 45 #	* 199 ± 4	91 ± 0.8	541 ± 18	**∞ 53 ± 0.4**	180 ± 1	∞ 57 ± 4
AHP3 + CP4 + CuO	*** 8879 ± 154** ^	---	*** 148 ± 1**	* 608 ± 17 ^	∞ 51 ± 0.2	154 ± 4	52 ± 2
CuO NP	* 2688 ± 11	*** 304 ± 2**	52 ± 1	500 ± 18	14 ± 0.5	---	∞ 59 ± 1

'---' indicates not determined values. Values are shown as mean ± standard deviation. The symbol '*' depicts statistically significant increases in values compared to the control treatment. The symbols 'x', '#', and '^' depict statistically significant increases in values compared to the AHP3, CP4, and AHP3 + CP4 treatments as controls, respectively (based on our ANOVA). The symbol '∞' indicates statistically significant increases in values compared to that of the control (based on an unpaired *t*-test). The values in bold indicate the best result for a nutrient compared to the control.

Table 2. Macro- and micronutrients in leaves of HD3086 wheat cultivar treated with different combinations of PGPB and nanoparticles.

	Mg [mg kg^{-1}]	Ca [mg kg^{-1}]	Mn [mg kg^{-1}]	Fe [mg kg^{-1}]	Cu [mg kg^{-1}]	Zn [mg kg^{-1}]	Se [mg kg^{-1}]
Control	2478 ± 7	161 ± 0.4	67 ± 0	518 ± 13	11 ± 0.4	197 ± 1.5	46 ± 0.8
AHP3	* 2563 ± 22	* 553 ± 2	68 ± 0.8	*** 1035 ± 96**	10 ± 0.3	---	104 ± 3
CP4	* 2633 ± 38	* 261 ± 2	49 ± 0.4	489 ± 26	8 ± 0.3	---	61 ± 3
AHP3 + CP4	* 2768 ± 40	187 ± 2	70 ± 1	532 ± 18	∞ 18 ± 0	44 ± 6	47 ± 2
AHP3 + MS	* 3747 ± 88 x	161 ± 0.4	57 ± 2	433 ± 18	9 ± 0.4	29 ± 2	46 ± 0.5
CP4 + MS	* 8368 ± 101 #	---	*** 203 ± 7** #	* 1010 ± 26 #	**∞ 51 ± 1**	*** 2277 ± 77**	79 ± 3
AHP3 + CP4 + MS	* 5341 ± 55 ^	* 348 ± 6 ^	103 ± 1	* 768 ± 18 ^	∞ 28 ± 0.8	---	93 ± 6
MS NP	* 4846 ± 69	152 ± 0.7	135 ± 2	* 795 ± 20	16 ± 0.7	5 ± 5	48 ± 2
AHP3 + ZnO	*** 9125 ± 42** x	---	* 180 ± 2 x	* 722 ± 12	∞ 33 ± 0.4	156 ± 6	54 ± 3
CP4 + ZnO	* 7754 ± 76 #	140 ± 2	110 ± 2	* 622 ± 12 #	∞ 22 ± 0.2	111 ± 4	* 165 ± 4 #
AHP3 + CP4 + ZnO	* 4241 ± 33 ^	156 ± 4	89 ± 2	531 ± 12	∞ 22 ± 0.5	88 ± 6	53 ± 0.7
ZnO NP	* 6523 ± 72	105 ± 4	90 ± 1	447 ± 28	∞ 22 ± 0.5	208 ± 13	47 ± 2
AHP3 + CuO	---	*** 1160 ± 3** x	20 ± 1	---	---	---	*** 333 ± 0.4** x
CP4 + CuO	* 4299 ± 72 #	* 300 ± 3	86 ± 0.5	499 ± 33	∞ 31 ± 0.6	* 459 ± 9 #	74 ± 5
AHP3 + CP4 + CuO	* 4591 ± 70 ^	* 708 ± 5 ^	75 ± 2	* 754 ± 17 ^	∞ 36 ± 1	* 929 ± 25 ^	* 150 ± 8 ^
CuO NP	* 4551 ± 79	154 ± 4	76 ± 2	378 ± 4	∞ 31 ± 0.1	230 ± 9	54 ± 3

Statistical significance and notations are as described in Table 1.

3.5. Post-Harvest Analysis Indicated Soil Health Improvement

3.5.1. Soil Organic Carbon

Post-harvest soil analysis revealed a notable enhancement across treated groups compared to the untreated control. The soil organic carbon (SOC) of black wheat soil showed significant improvement in all the treatments except the AHP3 + CP4 treatment. Particularly, the ZnO NP treatment exhibited the most significant advancement, reaching

a highest value of soil organic carbon (SOC) of 2.55 compared to the untreated control with a p-value < 0.0001 (Figure 9a). Furthermore, the combined application of PGPB and nanoparticles demonstrated a noteworthy increase in SOC when compared to PGPB alone, highlighting their synergistic effect. The exception was the CP4 + CuO treatment.

The HD3086 variety revealed noteworthy variations in SOC, with the CP4 + ZnO treatment causing a remarkable 528% increase compared to the untreated control (Figure 9b). Notably, the combinations of AHP3 + ZnO and CP4 + ZnO and ZnO alone demonstrated the most substantial increases compared to PGPB and other NP and PGPB combinations, with values of 2.85%, 3.83%, and 2.49%, respectively, with a p-value < 0.0001. When the MS treatment was taken as a control, CP4 alone with MS in black wheat and CP4 alone and in conjunction with AHP3 and MS in HD3086 showed a significant increase in soil organic carbon. When ZnO was taken as a control, AHP3 and CP4 alone with ZnO in HD3086 showed a significant increase in soil organic carbon. These findings align with current knowledge, highlighting the potential of specific nanoparticle and PGPB combinations to significantly enhance soil organic carbon. CP4 + ZnO, in particular, stands out for its substantial impact, suggesting its efficacy in promoting soil health. An increase in SOC is a crucial indicator of improved soil fertility and ecosystem resilience. Furthermore, the significant increase noted in the AHP3 + CP4 + CuO combination compared to AHP3 + CP4 (p-value < 0.001) adds nuance to the understanding of synergistic effects in soil management practices. These results point towards the practical applications of these treatments in sustainable agriculture, warranting further exploration and validation in diverse agricultural settings.

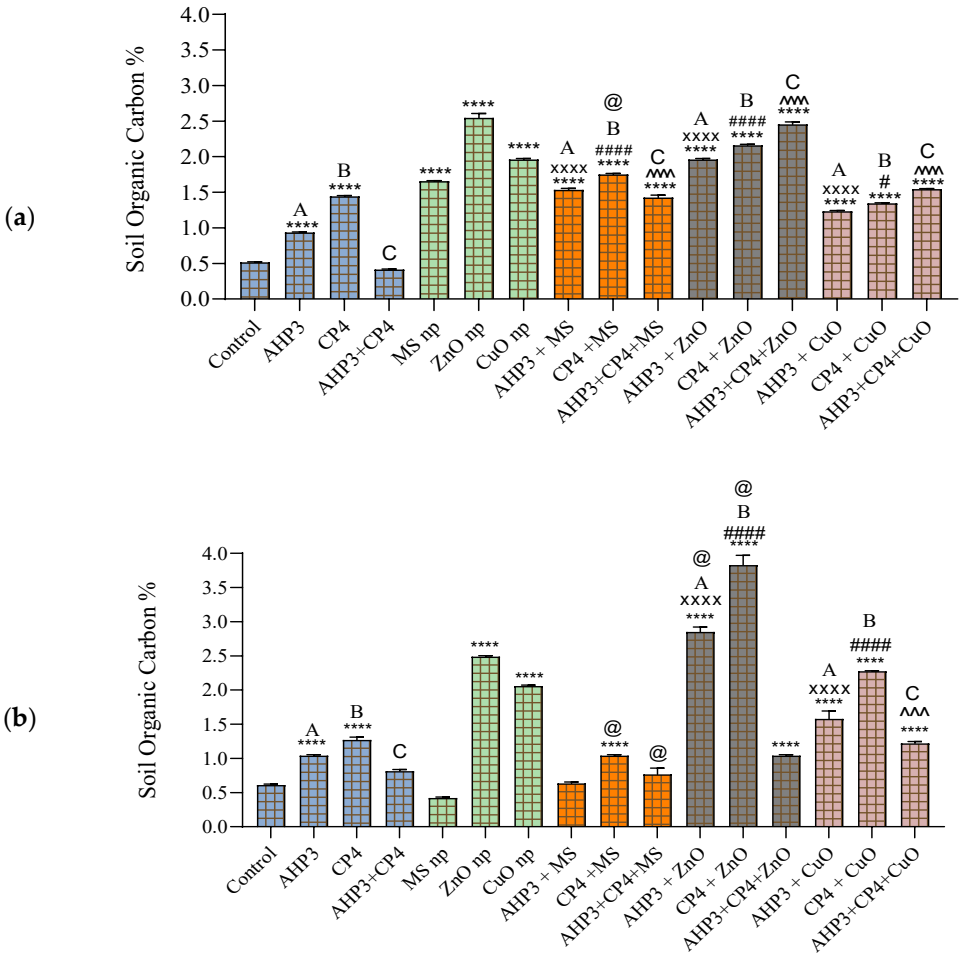

Figure 9. Soil organic carbon (SOC) at harvest stage in black wheat and HD3086 cultivars with different combinations of PGPB and nanoparticles. (**a**) Black wheat and (**b**) wheat variety HD3086. Annotations and statistical significance are as described in Figure 2.

3.5.2. Soil Invertase Activity

In the black wheat variety, the impact of the CP4 treatments was notably substantial, both when applied individually and in combination with MS and CuO NPs (Figure 10a). When compared to the consortia treatment used as a control, only the combination of CP4 with CuO NP demonstrated a significantly higher effect, registering a value of 996.7 μg g^{-1} 24 h^{-1} and a highly significant increase of 155.6%. Conversely, none of the treatments involving ZnO NPs showed a significant increase when compared to the control.

When the MS treatment was taken as a control, CP4 alone with MS NPs in black wheat and CP4 alone and consortium with AHP3 and MS NPs in HD3086 showed a significant increase in soil invertase activity. When ZnO was taken as a control, AHP3 and CP4 in conjunction with ZnO in HD3086 showed a significant increase in soil invertase activity. When CuO was taken as a control, CP4 alone and AHP3 and CP4 in conjunction with CuO in black wheat and AHP3 alone with CuO in HD3086 showed a significant increase in soil invertase activity. Among all the treatments, soil invertase activity was more profound in the HD3086 variety, with AHP3 treated with CuO NPs displaying the most significant impact, registering a value of 2075 μg g^{-1} 24 h^{-1} and a substantial 114% increase when compared with the control (Figure 10b). Notably, when using CP4 as the control, the only treatment that showed a significant increase was CP4 + MS, with a 60.5% increase, achieving a value of 1558 μg g^{-1} 24 h^{-1}. These findings highlight the specificity of each treatment's effects on soil invertase activity in the HD3086 variety. AHP3 treated with CuO NPs showcased a significant stimulation of invertase, indicating its potential role in enhancing soil enzymatic processes. The observed increase in CP4 + MS NPs further highlights the nuanced responses to specific treatments. These results contribute valuable insights into complex interactions, emphasizing the need for precision in tailoring agricultural practices to optimize soil enzyme activity.

(**a**)

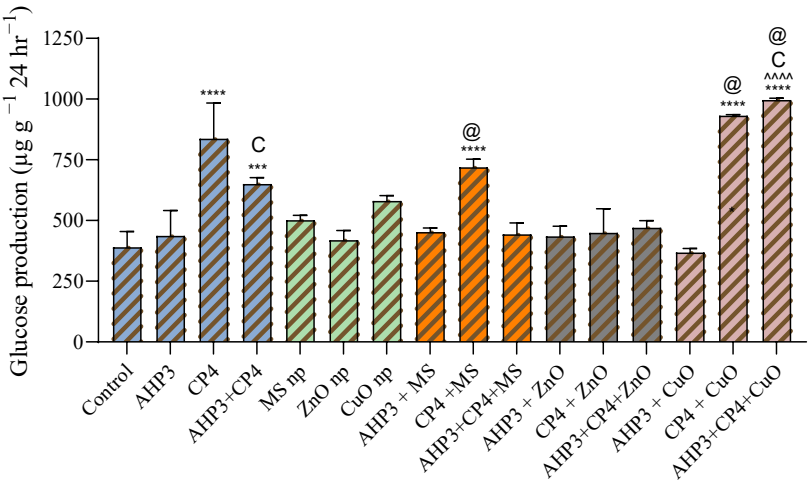

Figure 10. *Cont.*

(**b**)

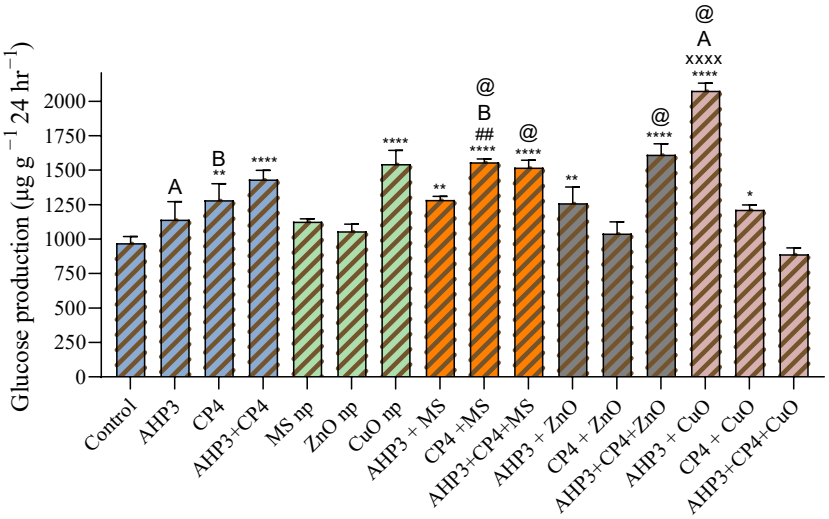

Figure 10. Soil enzyme invertase activity at harvest stage in black wheat and HD3086 plants with different combinations of PGPB and nanoparticles. (**a**) Black wheat and (**b**) wheat variety HD3086. Annotations and statistical significance are as described in Figure 2.

3.5.3. Soil Dehydrogenase Activity

Soil dehydrogenase activity acts as a proxy for endogenous respiration in soil. In the soil of the black wheat plants, when compared to the control, a highly significant increase was observed in AHP3 and CP4 with ZnO treatment and ZnO NPs alone and the combination of AHP3 and CP4 with CuO NPs (Figure 11a). The use of CP4 with the ZnO nanoparticles led to the highest increase of 107%, with a value of 8.8 TPF µg g^{-1} 24 h^{-1}. When AHP3 was taken as a control and compared with AHP3 and NPs, only AHP3 + ZnO showed a significant increase of 40.3%, with a value of 8.5 TPF µg g^{-1} 24 h^{-1}. Similarly, only the combination of CP4 with ZnO NPs showed a highly significant increase of 51.7% when CP4 was taken as a control. When the MS NP treatment was taken as a control, CP4 alone with MS NPs in black wheat showed a significant increase in soil dehydrogenase activity. When CuO was taken as a control, CP4 alone and AHP3 and CP4 in conjunction with CuO in black wheat showed a significant increase in soil dehydrogenase activity.

In HD3086, the ZnO NP treatments showed a highly significant increase of 94.5%, and the PGPB combinations with ZnO showed a highly significant increase of 93.8% in the AHP3 + ZnO treatment and 77.5% in the CP4 + ZnO treatment (Figure 11b) when compared to the control. The combination of AHP3 and CP4 with ZnO NPs also showed a significant improvement when compared to AHP3 and CP4 PGPB, with values of 145.4% and 83.7%, respectively. These results showed the varied responses of soil dehydrogenase activity to different PGPB and nanoparticle treatments in both black wheat and HD3086 soils. The substantial increases in dehydrogenase activity indicate positive impacts on soil microbial activity and organic matter decomposition. The differences observed in the treatments highlight the specificity of microbial responses to particular combinations, emphasizing the need for tailored soil management strategies in agricultural practices.

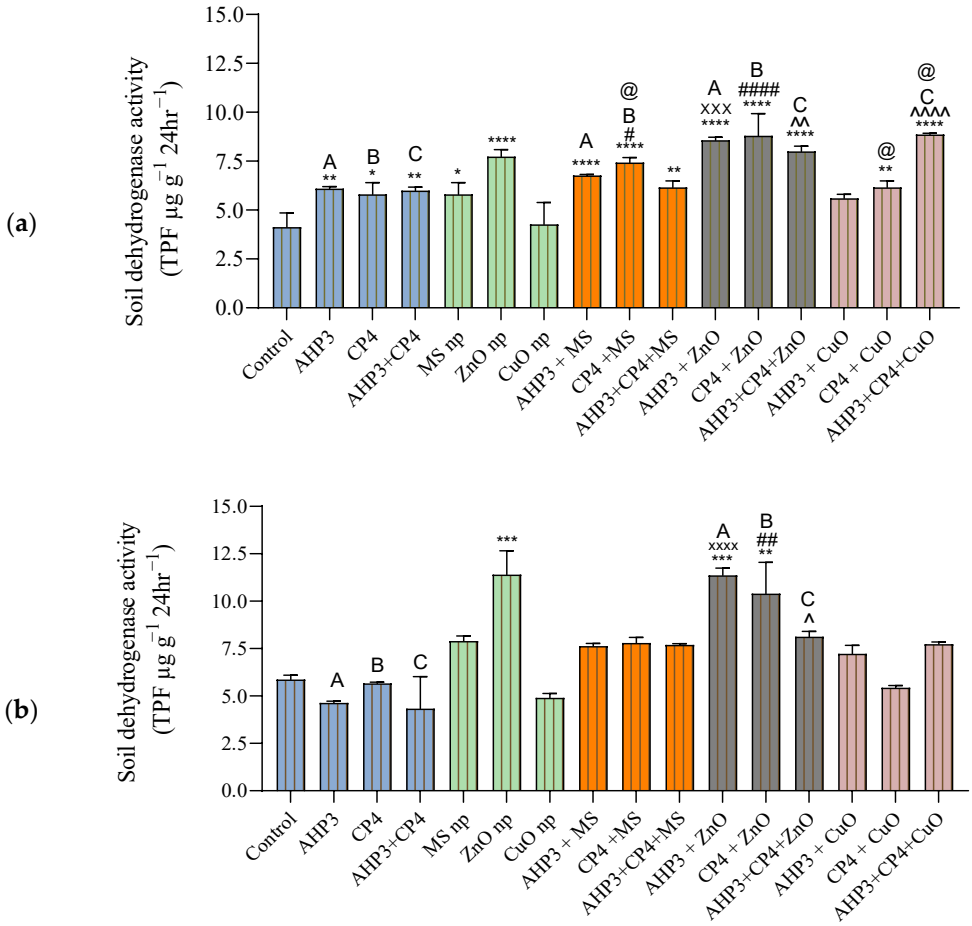

Figure 11. Soil enzyme dehydrogenase activity at harvest stage in black wheat and HD3086 with different combinations of PGPB and nanoparticles. (**a**) Black wheat and (**b**) wheat variety HD3086. Annotations and statistical significance are as described in Figure 2.

4. Discussion

The innovative approach of combining nanoparticles with plant growth-promoting bacteria is a relatively new concept for ecofriendly and sustainable agriculture. In our study, we observed that NPs and PGPB association with each other is mutually beneficial. Among the two PGPB and their combinations with three types of NP, the combination of ZnO NPs and biofertilizer exhibited superior effects on plant growth compared to the other two NP combinations. This was evidenced by the increases in root and shoot length, fresh weight, chlorophyll content, and protein content values. These findings align with previous studies wherein the application of ZnO NPs augmented plant growth-promoting traits [78,79]. While MS and CuO NP also promoted some plant growth traits, the trend in shoot and root length, as well as plant fresh weight, showed higher values for the black wheat variety than the HD3086 variety. In both varieties, a significant increase in shoot and root length was observed in the case of the ZnO NP treatment combined with the *Bacillus* species compared to the biofertilizer alone treatment. This suggests that nanobiofertilizers show an additive effect, combining the benefits of both biofertilizers and nanofertilizers. Previous studies have also highlighted the positive impact of both ZnO NPs and PGPB on wheat growth [51]. Moreover, CuO application decreased the root length and weight compared to the control plants. A similar result of decreased root length was reported in studies examining the dose-dependent application of CuO NP [73,80]. The significant increase in the fresh weight values seen in the black wheat plants treated with MS NPs in conjunction with *Bacillus* species may be attributed to the heightened cellular silica content, a crucial parameter for

plant growth [39]. Collectively, these observations contribute to our understanding of the nuanced effects of different nanoparticle and biofertilizer combinations on plant growth.

Chlorophyll content, a key indicator of crop growth and a direct measure of the photosynthetic capacity of leaves, forms the basis for the exchange of materials and energy between crops and their environment, providing valuable insights into crop health and development [81]. In our study, the total chlorophyll content was significantly increased in treatments involving the application of ZnO NPs alone and in conjunction with the *Bacillus* sp. for both wheat varieties. Zinc, an essential microelement, serves as a co-factor for pigment biosynthesis [82]. Consistent with our findings, Adil et al. [83] reported similar results, where treatment with increasing concentrations of ZnO NP enhanced the chlorophyll content in wheat leaves. Moreover, the treatments involving consortia with MS NP and MS NP alone showed an enhancement in total chlorophyll content. These results align with previous studies indicating a correlation between increased chlorophyll pigments and protein content, reflective of heightened photosynthetic activity [39]. Silica treatment has been shown to enhance the expression of genes related to the biosynthesis of chlorophyll, such as *PetH* and *PsbY*, which, in turn, enhance the activity of PS II, the rate of electron transfer, and the generation of NADPH [84]. These findings emphasize the intricate relationships between nanoparticle treatments and chlorophyll content, shedding light on the molecular mechanisms underlying enhanced photosynthetic activity. The results contribute to our understanding of how specific treatments influence key biochemical pathways, providing valuable insights for optimizing crop health and productivity in agriculture.

The total soluble protein content in both wheat varieties showed a significant increase upon treatment with ZnO and CuO NPs, either alone or in combination with bacteria. Zinc, an essential micronutrient for various physiological functions of plants, plays a major role in enzymatic activities and metabolic pathways, the synthesis of proteins, the transport of water, and membrane integrity [76]. Consistent with our findings, a previous study reported a significant increase in protein content and grain yield with the application of ZnO NPs with Zn biofertilizers [72].

Proline, a vital proteogenic amino acid, accumulates in plants in response to environmental stresses, serving multiple functions, such as regulating osmotic balance, combating free radicals, stabilizing subcellular structures, and maintaining cellular redox potential in response to stress [85]. In our study, a significant increase in the proline content of black wheat plants was observed with the CP4 + AHP3 treatment, as well as with the MS and CuO NPs treatments alone and with bacteria. The consortia with ZnO NP and AHP3 with the MS treatment exhibited the highest proline content in the HD3086 variety of wheat. These findings uncovered the influence of nanoparticle treatments, particularly the use of ZnO and CuO NPs, on crucial physiological aspects, such as protein and proline contents, in wheat varieties. The observed increases suggest benefits in terms of overall plant health.

Nitrogen, a crucial macronutrient for crop plants, plays a key role in vital processes such as growth, leaf expansion, and biomass yield production [86]. In our study, the nitrogen uptake increased in the HD3086 variety in all three NP treatment sets. Particularly, the treatment set with ZnO NPs and both bacteria showed a substantial increase in nitrogen in both wheat varieties. It was reported that the inoculation of *B. subtilis* and foliar fertilization with nano-Zn led to a significant increase in nitrogen biofortification, yield, and zinc use efficiency in wheat [87]. Additionally, the moderate supplementation of Zn to the rice plants was found to increase the activity of nitrate reductase and glutamine synthetase, thereby enhancing nitrogen synthesis [88].

In the case of phosphorus, an increase in uptake was observed in the leaves of HD3086 in the treatment with CuO and AHP3 and both bacterial isolates compared to the control. Conversely, the application of ZnO NPs to wheat plants decreased the phosphorus in the leaves, suggesting a reduced uptake of phosphorus from the soil to the shoot. Previous studies have proposed that this decline in phosphorus uptake may be attributed to the interaction of zinc with phosphorus, forming zinc phosphate, presumably in the phytate form, thereby hampering the bioavailability of zinc to plants [89]. These results highlight

the intricate dynamics of nutrient interactions influenced by nanoparticle treatments in different wheat varieties. The findings underscore the importance of considering nutrient bioavailability and potential interactions in nanoparticle-assisted nutrient management strategies for improved crop nutrition.

Macro- and micronutrient analysis in the leaves of both wheat varieties revealed a significant increase in Mg content in all treatments compared to the control. In the HD3086 variety, CP4 + MS exhibited the maximum levels of Mn, Cu, and Zn compared to the other treatments. In both wheat varieties, the amount of Cu in the leaf increased in all treatments with CuO NPs and bacteria except for the treatment involving the application of CuO NPs alone in black wheat. The Mn concentration in the ZnO and CuO NP treatments, alone and with bacteria, showed a higher value compared to the control in both wheat varieties. A previous study reported similar results, demonstrating an increase in Mn content when *Medicago polymorpha* L. plants were treated with ZnO and CuO [90]. However, plants treated with only CuO NP exhibited an increase in the uptake of Cu ions but a decrease in the uptake of other macro- and micronutrients, such as iron and calcium, in HD3086. This interference in Fe uptake may be attributed to the formation of a complex between Cu and 2′-deoxymugineic acid (DMA), a phytosiderophore. The level of the divalent cation Ca may be decreased due to its competition for uptake with CuO NP [80]. In plant roots, the antagonistic interactions between specific elements occur due to imbalances in relative nutrient concentration and the intense competition for the absorption by metal ion transporters localized in the roots. The direct application of the competing nutrient to aboveground parts of the plant does not cease this competition for nutrient uptake by the roots [91].

Soil analysis serves as a valuable tool for assessing a soil's potential to support plant growth, identifying deficits in essential nutrients necessary for plants, predicting fertilization needs, and evaluating the environmental risks associated with soil conditions [92]. Soil organic carbon, a crucial parameter for assessing soil fertility, was found to be at its highest in plants treated with ZnO and CuO nanoparticles in combination with bacteria in both wheat varieties. CuO nanoparticles have the potential to dissolve and release Cu ions, which can interact with the plant's root zone. The variables affecting the dissolution of CuO nanoparticles include dissolved soil organic matter, bacterial niches, and plant metabolic exudates [93]. In soil, invertase and dehydrogenase enzymes play essential roles in the carbon and nitrogen cycles. The current study demonstrated that the treatment with ZnO NPs alone and ZnO NPs and bacteria showed a significant increase in soil dehydrogenase activity in the soils of both wheat varieties. In black wheat, the combination of CuO and consortia also showed a significant increase in soil dehydrogenase activity. The *Bacillus* sp. CP4 treatment exhibited an increase in soil invertase activity compared to the control in the soils of both wheat varieties. Notably, the soil in the AHP3 + CuO treatment in the HD3086 variety showed a significant increase in invertase compared to the AHP3 alone treatment. These findings underscore the intricate interplay between nanoparticles, bacteria, and soil enzymes, contributing valuable insights into the complex dynamics of soil health and nutrient cycling in the context of agricultural practices.

The characteristics of NPs may be affected by various bioenvironmental conditions. As soil aggregation occurs, NP solubility is modified according to the coating or lack of coating of their surfaces by different plant and/or soil factors [94]. Microbial factors can also alter the bioactivity of nanoparticles. Extracellular polymeric substances (EPS) produced by *Bacillus* species are stimulated by Ag and ZnO nanoparticles, resulting in changes in the cellular processes to prevent toxicity [95]. Metallic nanoparticles (MNPs) interact intricately with biological and soil-associated factors, which include organic acids, sugars, proteins, ions, etc. NP or ions released by them modulate plant development and impede the growth of pathogens [96]. Root exudates of wheat influence the activity of CuO and ZnO NPs on the soil microbe *P. putida* KT2440, indicating a synergy with soil factors, which could serve as a protective mechanism for associated bacteria against the phytotoxic effects of NP [97].

The present study has shown the positive and variable effects of applying different nanoparticles alone and in combination with PGPB on morphological, physiological, and biochemical parameters related to plant growth. Although the use of nanoparticles alone had a positive effect on plant growth-promoting attributes, 31 out of 72 comparisons (43%) in black wheat and 27 out of 72 comparisons (38%) in HD3086 showed significant improvements in shoot length, root length, fresh weight, chlorophyll content, protein content, proline content, nitrogen, and phosphorus in the NP + PGPB treatment compared to NP-only treatment based on our ANOVA and/or *t*-tests. Similarly, 9 out of 27 comparisons (33%) in black wheat and 13 out of 27 comparisons (48%) in HD3086 showed significant improvements in soil organic carbon and soil dehydrogenase and invertase activities in the NP + PGPB treatment compared to NP-only treatment. Although most of the previous studies in the literature have reported positive effects derived from the use of nanoparticles such as CuO, ZnO, and TiO_2 NPs on plant growth-related parameters, aligning with our studies, there are some studies that have reported a decrease in plant growth-related parameters with the use of nanoparticles [73,98]. These contrasting results may be attributed to a number of factors, including plant species/genotype, growth conditions, nature of nanoparticles, nature of soil, and environment/climate.

5. Conclusions

The application of nanoparticles in conjunction with PGPB, employed as nanobiofertilizers, exhibited an overall improvement in plant growth parameters and soil health compared to the control. About one-third to half of the treatments involving both NPs and PGPB showed significant improvement in wheat growth-promoting attributes and soil health compared to NP treatment as a control. The findings of the current study highlighted that zinc oxide nanoparticles, when combined with bacteria, augmented plant growth the most by exerting a positive influence on morphological and growth traits, including shoot and root lengths and chlorophyll, protein, and nitrogen contents. Additionally, mesoporous silica nanoparticles enhanced chlorophyll contents, along with the contents of proline and nitrogen. The integration of nanotechnology in agriculture in the form of nanobiofertilizers could emerge as an effective tool to improve agriculture if delivered in an economical and sustainable manner.

Author Contributions: A.K., Y.F. and P.S. performed experiments, data analysis, and wrote the initial draft of the manuscript. R.B. performed some experiments and helped with technical support. J.S. carried out the designing of the experiments, data analysis, and supervision. W.R. prepared the work plan, carried out supervision, and revised and prepared the final version of the manuscript. All authors have read and agreed to the published version of the manuscript.

Funding: The authors acknowledge funding by DST-FIST (sanction order number SR/FST/LS-I/2018/125(C)). Junior and senior fellowship to R.B. was funded by the Council of Scientific and Industrial Research (CSIR), New Delhi, India.

Institutional Review Board Statement: Not applicable.

Data Availability Statement: Data is contained within the article. The data presented in this study are available in article.

Acknowledgments: We acknowledge Monika Garg, Scientist, National Agri-Food. Biotechnology Institute (NABI), Mohali, India, for providing seeds of black wheat and Achla Sharma, Principal Wheat Breeder, Punjab Agricultural University (PAU), Ludhiana, India, for providing wheat seeds of the HD3086 variety. CIL is acknowledged for their help in ICP-MS analysis.

Conflicts of Interest: The authors declare no conflicts of interest.

References

1. Chaudhary, P.; Singh, S.; Chaudhary, A.; Sharma, A.; Kumar, G. Overview of biofertilizers in crop production and stress management for sustainable agriculture. *Front. Plant Sci.* **2022**, *13*, 930340. [CrossRef] [PubMed]

2. Kumar, S.; Diksha Sindhu, S.S.; Kumar, R. Biofertilizers: An ecofriendly technology for nutrient recycling and environmental sustainability. *Curr. Res. Microb. Sci.* **2022**, *3*, 100094. [CrossRef]
3. Bhardwaj, D.; Ansari, M.W.; Sahoo, R.K.; Tuteja, N. Biofertilizers function as key player in sustainable agriculture by improving soil fertility, plant tolerance and crop productivity. *Microb. Cell Fact.* **2014**, *13*, 66. [CrossRef] [PubMed]
4. Glick, B.R. *Beneficial Plant-Bacterial Interactions*; Springer: Berlin/Heidelberg, Germany, 2015; p. 243.
5. Vejan, P.; Abdullah, R.; Khadiran, T.; Ismail, S.; Nasrulhaq Boyce, A. Role of plant growth promoting rhizobacteria in agricultural sustainability—A review. *Molecules* **2016**, *21*, 573. [CrossRef]
6. Olanrewaju, O.S.; Glick, B.R.; Babalola, O.O. Mechanisms of action of plant growth promoting bacteria. *World J. Microbiol. Biotechnol.* **2017**, *33*, 197. [CrossRef] [PubMed]
7. Abebe, T.G.; Tamtam, M.R.; Abebe, A.A.; Abtemariam, K.A.; Shigut, T.G.; Dejen, Y.A.; Haile, E.G. Growing use and impacts of chemical fertilizers and assessing alternative organic fertilizer sources in Ethiopia. *Appl. Environ. Soil Sci.* **2022**, *2022*, 4738416. [CrossRef]
8. Adesemoye, A.O.; Kloepper, J.W. Plant-microbes interactions in enhanced fertilizer-use efficiency. *Appl. Microbiol. Biotechnol.* **2009**, *85*, 1–12. [CrossRef]
9. Tsolakidou, M.-D.; Stringlis, I.A.; Fanega-Sleziak, N.; Papageorgiou, S.; Tsalakou, A.; Pantelides, I.S. Rhizosphere-enriched microbes as a pool to design synthetic communities for reproducible beneficial outputs. *FEMS Microbiol. Ecol.* **2019**, *95*, fiz138. [CrossRef]
10. Khan, M.; Salman, M.; Jan, S.A.; Shinwari, Z.K. Biological control of fungal phytopathogens: A comprehensive review based on *Bacillus* species. *MedCrave Online J. Biol. Med.* **2021**, *6*, 90–92. [CrossRef]
11. Ferreira, C.M.; Vilas-Boas, Â.; Sousa, C.A.; Soares, H.M.; Soares, E.V. Comparison of five bacterial strains producing siderophores with ability to chelate iron under alkaline conditions. *AMB Express* **2019**, *9*, 78. [CrossRef]
12. Yadav, R.; Ror, P.; Rathore, P.; Ramakrishna, W. Bacteria from native soil in combination with arbuscular mycorrhizal fungi augment wheat yield and biofortification. *Plant Physiol. Biochem.* **2020**, *150*, 222–233. [CrossRef] [PubMed]
13. Duhan, J.S.; Kumar, R.; Kumar, N.; Kaur, P.; Nehra, K.; Duhan, S. Nanotechnology: The new perspective in precision agriculture. *Biotechnol. Rep.* **2017**, *15*, 11–23. [CrossRef] [PubMed]
14. Dimkpa, C.O.; Bindraban, P.S. Nanofertilizers. New products for the industry? *J. Agric. Food Chem.* **2017**, *66*, 6462–6473. [CrossRef] [PubMed]
15. Akhtar, N.; Ilyas, N.; Meraj, T.A.; Pour-Aboughadareh, A.; Sayyed, R.; Mashwani, Z.-u.-R.; Poczai, P. Improvement of plant responses by nanobiofertilizer: A step towards sustainable agriculture. *Nanomaterials* **2022**, *12*, 965. [CrossRef]
16. Kumari, R.; Singh, D.P. Nano-biofertilizer: An emerging eco-friendly approach for sustainable agriculture. *Proc. Natl. Acad. Sci. India Sect. B Biol. Sci.* **2020**, *90*, 733–741. [CrossRef]
17. de Moraes, A.C.P.; Ribeiro, L.d.S.; de Camargo, E.R.; Lacava, P.T. The potential of nanomaterials associated with plant growth-promoting bacteria in agriculture. *3 Biotech* **2021**, *11*, 318. [CrossRef]
18. Vedamurthy, A.; Bhattacharya, S.; Das, A.; Shruthi, S. Exploring nanomaterials with rhizobacteria in current agricultural scenario. In *Advances in Nano-Fertilizers and Nano-Pesticides in Agriculture*; Elsevier: Amsterdam, The Netherlands, 2021; pp. 487–503.
19. Jogaiah, S.; Singh, H.B.; Fraceto, L.F.; De Lima, R. *Advances in Nano-Fertilizers and Nano-Pesticides in Agriculture: A Smart Delivery System for Crop Improvement*; Woodhead Publishing: Sawston, UK, 2020; p. 650.
20. Hayden, S.C.; Zhao, G.; Saha, K.; Phillips, R.L.; Li, X.; Miranda, O.R.; Rotello, V.M.; El-Sayed, M.A.; Schmidt-Krey, I.; Bunz, U.H. Aggregation and interaction of cationic nanoparticles on bacterial surfaces. *J. Am. Chem. Soc.* **2012**, *134*, 6920–6923. [CrossRef]
21. Dinesh, R.; Anandaraj, M.; Srinivasan, V.; Srambikkal, H. Engineered nanoparticles in the soil and their potential implications to microbial activity. *Geoderma* **2012**, *173–174*, 19–27. [CrossRef]
22. Jiang, W.; Yang, K.; Vachet, R.W.; Xing, B. Interaction between oxide nanoparticles and biomolecules of the bacterial cell envelope as examined by infrared spectroscopy. *Langmuir* **2010**, *26*, 18071–18077. [CrossRef] [PubMed]
23. Abarzua, S.; Jakubowski, S. Biotechnological investigation for the prevention of biofouling. I. Biological and biochemical principles for the prevention of biofouling. *Mar. Ecol. Prog. Ser.* **1995**, *123*, 301–312. [CrossRef]
24. Tang, H.; Wang, A.; Liang, X.; Cao, T.; Salley, S.O.; McAllister, J.P., III; Ng, K.S. Effect of surface proteins on *Staphylococcus epidermidis* adhesion and colonization on silicone. *Colloids Surf. B Biointerfaces* **2006**, *51*, 16–24. [CrossRef]
25. Dimkpa, C.O.; McLean, J.E.; Britt, D.W.; Anderson, A.J. CuO and ZnO nanoparticles differently affect the secretion of fluorescent siderophores in the beneficial root colonizer, *Pseudomonas chlororaphis* O6. *Nanotoxicology* **2012**, *6*, 635–642. [CrossRef]
26. Dimkpa, C.O.; Zeng, J.; McLean, J.E.; Britt, D.W.; Zhan, J.; Anderson, A.J. Production of indole-3-acetic acid via the indole-3-acetamide pathway in the plant-beneficial bacterium *Pseudomonas chlororaphis* O6 is inhibited by ZnO nanoparticles but enhanced by CuO nanoparticles. *Appl. Environ. Microbiol.* **2012**, *78*, 1404–1410. [CrossRef] [PubMed]
27. Guan, X.; Gao, X.; Avellan, A.; Spielman-Sun, E.; Xu, J.; Laughton, S.; Yun, J.; Zhang, Y.; Bland, G.D.; Zhang, Y.; et al. CuO nanoparticles alter the rhizospheric bacterial community and local nitrogen cycling for wheat grown in a calcareous soil. *Environ. Sci. Technol.* **2020**, *54*, 8699–8709. [CrossRef] [PubMed]
28. Elmer, W.; De La Torre-Roche, R.; Pagano, L.; Majumdar, S.; Zuverza-Mena, N.; Dimkpa, C.; Gardea-Torresdey, J.; White, J.C. Effect of Metalloid and Metal Oxide Nanoparticles on Fusarium Wilt of Watermelon. *Plant Dis.* **2018**, *102*, 1394–1401. [CrossRef]
29. Djamin, A.; Pathak, M.D. Role of silica in resistance to Asiatic rice borer, *Chilo suppressalis* (Walker), in rice varieties. *J. Econ. Entomol.* **1967**, *60*, 347–351. [CrossRef]

30. Kaufman, P.B.; Takeoka, Y.; Carlson, T.J.; Bigelow, W.C.; Jones, J.; Moore, P.; Ghosheh, N. Studies on silica deposition in sugarcane (*Saccharum* spp.) using scanning electron microscopy, energy-dispersive X-ray analysis, neutron activation analysis, and light microscopy. *Phytomorphology* **1979**, *29*, 185–193.
31. Cui, J.; Li, Y.; Jin, Q.; Li, F. Silica nanoparticles inhibit arsenic uptake into rice suspension cells via improving pectin synthesis and the mechanical force of the cell wall. *Environ. Sci. Nano* **2020**, *7*, 162–171. [CrossRef]
32. Karunakaran, G.; Suriyaprabha, R.; Manivasakan, P.; Yuvakkumar, R.; Rajendran, V.; Prabu, P.; Kannan, N. Effect of nanosilica and silicon sources on plant growth promoting rhizobacteria, soil nutrients and maize seed germination. *IET Nanobiotechnol.* **2013**, *7*, 70–77. [CrossRef]
33. Gordienko, A.S.; Kurdish, I.K. Surface electrical properties of *Bacillus subtilis* cells and the effect of interaction with silicon dioxide particles. *Biophysics* **2007**, *52*, 217–219. [CrossRef]
34. Hirota, R.; Hata, Y.; Ikeda, T.; Ishida, T.; Kuroda, A. The silicon layer supports acid resistance of *Bacillus cereus* spores. *J. Bacteriol.* **2010**, *192*, 111–116. [CrossRef] [PubMed]
35. Akter, N.; Rafiqul Islam, M. Heat stress effects and management in wheat. A review. *Agron. Sustain. Dev.* **2017**, *37*, 37. [CrossRef]
36. Singh, G.P.; Prabhu, K.V.; Singh, P.K.; Singh, A.M.; Jain, N.; Ramya, P.; Sharma, J.B.; Kumar, J.; Siwasami, M.; Prasad, S.S.; et al. HD 3086: A new wheat variety for irrigated, timely sown condition of North Western Plains Zone of India. *J. Wheat Res.* **2014**, *6*, 179–180.
37. Singh, K.; Madhusudanan, M.; Verma, A.K.; Kumar, C.; Ramawat, N. Engineered zinc oxide nanoparticles: An alternative to conventional zinc sulphate in neutral and alkaline soils for sustainable wheat production. *3 Biotech* **2021**, *11*, 322. [CrossRef]
38. Haider, H.I.; Zafar, I.; Ain, Q.u.; Noreen, A.; Nazir, A.; Javed, R.; Sehgal, S.A.; Khan, A.A.; Rahman, M.M.; Rashid, S.; et al. Synthesis and characterization of copper oxide nanoparticles: Its influence on corn (*Z. mays*) and wheat (*Triticum aestivum*) plants by inoculation of *Bacillus subtilis*. *Environ. Sci. Pollut. Res.* **2023**, *30*, 37370–37385. [CrossRef]
39. Sun, D.; Hussain, H.I.; Yi, Z.; Rookes, J.E.; Kong, L.; Cahill, D.M. Mesoporous silica nanoparticles enhance seedling growth and photosynthesis in wheat and lupin. *Chemosphere* **2016**, *152*, 81–91. [CrossRef]
40. Garg, M.; Chawla, M.; Chunduri, V.; Kumar, R.; Sharma, S.; Sharma, N.K.; Sharma, N.K.; Kaur, N.; Kumar, A.; Mundey, J.K.; et al. Transfer of grain colors to elite wheat cultivars and their characterization. *J. Cereal Sci.* **2016**, *71*, 138–144. [CrossRef]
41. Li, W.; Beta, T.; Sun, S.; Corke, H. Protein characteristics of Chinese black-grained wheat. *Food Chem.* **2006**, *98*, 463–472. [CrossRef]
42. Liu, R.H. Whole grain phytochemicals and health. *J. Cereal Sci.* **2007**, *46*, 207–219. [CrossRef]
43. Dykes, L.; Rooney, L. Phenolic compounds in cereal grains and their health benefits. *Cereal Foods World* **2007**, *52*, 105–111. [CrossRef]
44. Kaur, S.; Kumari, A.; Sharma, N.; Pandey, A.K.; Garg, M. Physiological and molecular response of colored wheat seedlings against phosphate deficiency is linked to accumulation of distinct anthocyanins. *Plant Physiol. Biochem.* **2022**, *170*, 338–349. [CrossRef]
45. Cappuccino, J.; Sherman, N. *Microbiology: A Laboratory Manual*; Benjamin/Cummings Publishing Co.: New York, NY, USA, 1992; pp. 125–179.
46. Lorck, H. Production of hydrocyanic acid by bacteria. *Physiol. Plant.* **1948**, *1*, 142–146. [CrossRef]
47. Reiner, K. *Catalase Test Protocol*; American Society for Microbiology: Washington, DC, USA, 2010; pp. 1–6.
48. Sivolapov, P.; Myronyuk, O.; Baklan, D. Synthesis of Stober silica nanoparticles in solvent environments with different Hansen solubility parameters. *Inorg. Chem. Commun.* **2022**, *143*, 109769. [CrossRef]
49. Nazir, S.; Zaka, M.; Adil, M.; Abbasi, B.H.; Hano, C. Synthesis, characterisation and bactericidal effect of ZnO nanoparticles via chemical and bio-assisted (*Silybum marianum* in vitro plantlets and callus extract) methods: A comparative study. *IET Nanobiotechnol.* **2018**, *12*, 604–608. [CrossRef]
50. Phiwdang, K.; Suphankij, S.; Mekprasart, W.; Pecharapa, W. Synthesis of CuO nanoparticles by precipitation method using different precursors. *Energy Procedia* **2013**, *34*, 740–745. [CrossRef]
51. Seyed Sharifi, R.; Khalilzadeh, R.; Pirzad, A.; Anwar, S. Effects of biofertilizers and nano zinc-iron oxide on yield and physico-chemical properties of wheat under water deficit conditions. *Commun. Soil Sci. Plant Anal.* **2020**, *51*, 2511–2524. [CrossRef]
52. Yadav, R.; Ror, P.; Beniwal, R.; Kumar, S.; Ramakrishna, W. *Bacillus* sp. and arbuscular mycorrhizal fungi consortia enhance wheat nutrient and yield in the second-year field trial: Superior performance in comparison with chemical fertilizers. *J. Appl. Microbiol.* **2022**, *132*, 2203–2219. [CrossRef] [PubMed]
53. Gupta, P.; Srivastava, S.; Seth, C.S. 24-Epibrassinolide and sodium nitroprusside alleviate the salinity stress in *Brassica juncea* L. cv. Varuna through cross talk among proline, nitrogen metabolism and abscisic acid. *Plant Soil* **2017**, *411*, 483–498. [CrossRef]
54. Arnon, D.I. Copper enzymes in isolated chloroplasts. Polyphenoloxidase in *Beta vulgaris*. *Plant Physiol.* **1949**, *24*, 1–15. [CrossRef]
55. Bradford, M.M. A rapid and sensitive method for the quantitation of microgram quantities of protein utilizing the principle of protein-dye binding. *Anal. Biochem.* **1976**, *72*, 248–254. [CrossRef] [PubMed]
56. Rodger, A.; Sanders, K. Biomacromolecular Applications of UV-Visible Absorption Spectroscopy. In *Encyclopedia of Spectroscopy and Spectrometry*, 3rd ed.; Lindon, J.C., Tranter, G.E., Koppenaal, D.W., Eds.; Academic Press: Cambridge, MA, USA, 2017; pp. 495–502.
57. Guy, C.; Haskell, D.; Neven, L.; Klein, P.; Smelser, C. Hydration-state-responsive proteins link cold and drought stress in spinach. *Planta* **1992**, *188*, 265–270. [CrossRef] [PubMed]
58. Bates, L.; Waldren, R.A.; Teare, I. Rapid determination of free proline for water-stress studies. *Plant Soil* **1973**, *39*, 205–207. [CrossRef]

59. Flindt, M.R.; Lillebø, A.I. Determination of total nitrogen and phosphorus in leaf litter. In *Methods to Study Litter Decomposition*; Graça, M.A., Bärlocher, F., Gessner, M.O., Eds.; Springer: Dordrecht, The Netherlands, 2005; pp. 53–59.
60. Lindner, R. Rapid analytical methods for some of the more common inorganic constituents of plant tissues. *Plant Physiol.* **1944**, *19*, 76–89. [CrossRef] [PubMed]
61. Dogra, N.; Yadav, R.; Kaur, M.; Adhikary, A.; Kumar, S.; Ramakrishna, W. Nutrient enhancement of chickpea grown with plant growth promoting bacteria in local soil of Bathinda, Northwestern India. *Physiol. Mol. Biol. Plants* **2019**, *25*, 1251–1259. [CrossRef] [PubMed]
62. Schumacher, B.A. *Methods for the Determination of Total Organic Carbon (TOC) in Soils and Sediments*; Ecological Risk Assessment Support Center, Office of Research and Development, US Environmental Protection Agency: Washington, DC, USA, 2002; pp. 1–23.
63. Walkley, A. A critical examination of a rapid method for determining organic carbon in soils—Effect of variations in digestion conditions and of inorganic soil constituents. *Soil Sci.* **1947**, *63*, 251–264. [CrossRef]
64. Skujins, J.J.; Braal, L.; McLaren, A.D. Characterization of phosphatase in a terrestrial soil sterilized with an electron beam. *Enzymologia* **1962**, *25*, 125–133.
65. Frankeberger, W.; Johanson, J. Method of measuring invertase activity in soils. *Plant Soil* **1983**, *74*, 301–311. [CrossRef]
66. Casida Jr, L.; Klein, D.A.; Santoro, T. Soil dehydrogenase activity. *Soil Sci.* **1964**, *98*, 371–376. [CrossRef]
67. Bhattacharyya, C.; Banerjee, S.; Acharya, U.; Mitra, A.; Mallick, I.; Haldar, A.; Haldar, S.; Ghosh, A.; Ghosh, A. Evaluation of plant growth promotion properties and induction of antioxidative defense mechanism by tea rhizobacteria of Darjeeling, India. *Sci. Rep.* **2020**, *10*, 15536. [CrossRef]
68. Sehrawat, A.; Sindhu, S.S.; Glick, B.R. Hydrogen cyanide production by soil bacteria: Biological control of pests and promotion of plant growth in sustainable agriculture. *Pedosphere* **2022**, *32*, 15–38. [CrossRef]
69. Das, P.; Nutan, K.K.; Singla-Pareek, S.L.; Pareek, A. Oxidative environment and redox homeostasis in plants: Dissecting out significant contribution of major cellular organelles. *Front. Environ. Sci.* **2015**, *2*, 70. [CrossRef]
70. Du, W.; Yang, J.; Peng, Q.; Liang, X.; Mao, H. Comparison study of zinc nanoparticles and zinc sulphate on wheat growth: From toxicity and zinc biofortification. *Chemosphere* **2019**, *227*, 109–116. [CrossRef]
71. Yadav, R.; Ror, P.; Rathore, P.; Kumar, S.; Ramakrishna, W. *Bacillus subtilis* CP4, isolated from native soil in combination with arbuscular mycorrhizal fungi promotes biofortification, yield and metabolite production in wheat under field conditions. *J. Appl. Microbiol.* **2021**, *131*, 339–359. [CrossRef]
72. Saleem, S.; Malik, A.; Khan, S.T. ZnO nanoparticles in combination with Zn biofertilizer improve wheat plant growth and grain Zn content without significantly changing the rhizospheric microbiome. *Environ. Exp. Bot.* **2023**, *213*, 105446. [CrossRef]
73. Bai, T.; Zhang, P.; Guo, Z.; Chetwynd, A.J.; Zhang, M.; Adeel, M.; Li, M.; Guo, K.; Gao, R.; Li, J.; et al. Different physiological responses of C3 and C4 plants to nanomaterials. *Environ. Sci. Pollut. Res.* **2021**, *28*, 25542–25551. [CrossRef]
74. Chen, G.; Li, J.; Han, H.; Du, R.; Wang, X. Physiological and molecular mechanisms of plant responses to copper stress. *Int. J. Mol. Sci.* **2022**, *23*, 12950. [CrossRef]
75. Gonzalez, D.J.; Haste, N.M.; Hollands, A.; Fleming, T.C.; Hamby, M.; Pogliano, K.; Nizet, V.; Dorrestein, P.C. Microbial competition between *Bacillus subtilis* and *Staphylococcus aureus* monitored by imaging mass spectrometry. *Microbiology* **2011**, *157 Pt 9*, 2485–2492. [CrossRef] [PubMed]
76. Hafeez, B.; Khanif, Y.; Saleem, M. Role of zinc in plant nutrition-a review. *Am. J. Exp. Agric.* **2013**, *3*, 374–391. [CrossRef]
77. Hafeez, A.; Razzaq, A.; Mahmood, T.; Jhanzab, H.M. Potential of copper nanoparticles to increase growth and yield of wheat. *J. Nanosci. Adv. Technol.* **2015**, *1*, 6–11.
78. Munir, T.; Rizwan, M.; Kashif, M.; Shahzad, A.; Ali, S.; Amin, N.; Zahid, R.; Alam, M.F.E.; Imran, M. Effect of zinc oxide nanoparticles on the growth and Zn uptake in wheat (*Triticum aestivum* L.) by seed priming method. *Dig. J. Nanomater. Biostruct.* **2018**, *13*, 315.
79. Dimkpa, C.O.; Singh, U.; Bindraban, P.S.; Elmer, W.H.; Gardea-Torresdey, J.L.; White, J.C. Exposure to weathered and fresh nanoparticle and ionic Zn in soil promotes grain yield and modulates nutrient acquisition in wheat (*Triticum aestivum* L.). *J. Agric. Food Chem.* **2018**, *66*, 9645–9656. [CrossRef] [PubMed]
80. McManus, P.; Hortin, J.; Anderson, A.J.; Jacobson, A.R.; Britt, D.W.; Stewart, J.; McLean, J.E. Rhizosphere interactions between copper oxide nanoparticles and wheat root exudates in a sand matrix: Influences on copper bioavailability and uptake. *Environ. Toxicol. Chem.* **2018**, *37*, 2619–2632. [CrossRef] [PubMed]
81. Shi, H.; Guo, J.; An, J.; Tang, Z.; Wang, X.; Li, W.; Zhao, X.; Jin, L.; Xiang, Y.; Li, Z.; et al. Estimation of chlorophyll content in soybean crop at different growth stages based on optimal spectral index. *Agronomy* **2023**, *13*, 663. [CrossRef]
82. Balashouri, P.; Prameeladevi, Y. Effect of zinc on germination, growth and pigment content and phytomass of *Vigna radiata* and *Sorghum bicolor*. *J. Ecobiol.* **1995**, *7*, 109–114.
83. Adil, M.; Bashir, S.; Bashir, S.; Aslam, Z.; Ahmad, N.; Younas, T.; Asghar, R.M.A.; Alkahtani, J.; Dwiningsih, Y.; Elshikh, M.S. Zinc oxide nanoparticles improved chlorophyll contents, physical parameters, and wheat yield under salt stress. *Front. Plant Sci.* **2022**, *13*, 932861. [CrossRef]
84. Song, A.; Li, P.; Fan, F.; Li, Z.; Liang, Y. The effect of silicon on photosynthesis and expression of its relevant genes in rice (*Oryza sativa* L.) under high-zinc stress. *PLoS ONE* **2014**, *9*, e113782. [CrossRef]

85. Ashraf, M.; Foolad, M.R. Roles of glycine betaine and proline in improving plant abiotic stress resistance. *Environ. Exp. Bot.* **2007**, *59*, 206–216. [CrossRef]
86. Anas, M.; Liao, F.; Verma, K.K.; Sarwar, M.A.; Mahmood, A.; Chen, Z.-L.; Li, Q.; Zeng, X.-P.; Liu, Y.; Li, Y.-R. Fate of nitrogen in agriculture and environment: Agronomic, eco-physiological and molecular approaches to improve nitrogen use efficiency. *Biol. Res.* **2020**, *53*, 47. [CrossRef]
87. Jalal, A.; Oliveira, C.E.d.S.; Fernandes, G.C.; da Silva, E.C.; da Costa, K.N.; de Souza, J.S.; Leite, G.d.S.; Biagini, A.L.C.; Galindo, F.S.; Teixeira Filho, M.C.M. Integrated use of plant growth-promoting bacteria and nano-zinc foliar spray is a sustainable approach for wheat biofortification, yield, and zinc use efficiency. *Front. Plant Sci.* **2023**, *14*, 1146808. [CrossRef] [PubMed]
88. Wang, R.; Mi, K.; Yuan, X.; Chen, J.; Pu, J.; Shi, X.; Yang, Y.; Zhang, H.; Zhang, H. Zinc oxide nanoparticles foliar application effectively enhanced zinc and aroma content in rice (*Oryza sativa* L.) grains. *Rice* **2023**, *16*, 36. [CrossRef] [PubMed]
89. Dimkpa, C.O.; White, J.C.; Elmer, W.H.; Gardea-Torresdey, J. Nanoparticle and ionic Zn promote nutrient loading of sorghum grain under low NPK fertilization. *J. Agric. Food Chem.* **2017**, *65*, 8552–8559. [CrossRef]
90. Ji, H.; Guo, Z.; Wang, G.; Wang, X.; Liu, H. Effect of ZnO and CuO nanoparticles on the growth, nutrient absorption, and potential health risk of the seasonal vegetable *Medicago polymorpha* L. *PeerJ* **2022**, *10*, e14038. [CrossRef]
91. Dimkpa, C.O.; Bindraban, P.S.; Fugice, J.; Agyin-Birikorang, S.; Singh, U.; Hellums, D. Composite micronutrient nanoparticles and salts decrease drought stress in soybean. *Agron. Sustain. Dev.* **2017**, *37*, 5. [CrossRef]
92. Peverill, K.I.; Sparrow, L.; Reuter, D.J. *Soil Analysis: An Interpretation Manual*; CSIRO Publishing: Clayton, Australia, 1999.
93. Hortin, J.; Anderson, A.; Britt, D.; Jacobson, A.; McLean, J. Copper oxide nanoparticle dissolution at alkaline pH is controlled by dissolved organic matter: Influence of soil-derived organic matter, wheat, bacteria, and nanoparticle coating. *Environ. Sci. Nano* **2020**, *7*, 2618–2631. [CrossRef]
94. Wu, H.; Li, Z. Nano-enabled agriculture: How do nanoparticles cross barriers in plants? *Plant Commun.* **2022**, *3*, 100346. [CrossRef]
95. Raliya, R.; Tarafdar, J.C.; Mahawar, H.; Kumar, R.; Gupta, P.; Mathur, T.; Kaul, R.K.; Praveen-Kumar Kalia, A.; Gautam, R.; Singh, S.K.; et al. ZnO nanoparticles induced exopolysaccharide production by *B. subtilis* strain JCT1 for arid soil applications. *Int. J. Biol. Macromol.* **2014**, *65*, 362–368. [CrossRef] [PubMed]
96. Mittal, D.; Kaur, G.; Singh, P.; Yadav, K.; Ali, S.A. Nanoparticle-based sustainable agriculture and food science: Recent advances and future outlook. *Front. Nanotechnol.* **2020**, *2*, 579954. [CrossRef]
97. Martineau, N.; McLean, J.E.; Dimkpa, C.O.; Britt, D.W.; Anderson, A.J. Components from wheat roots modify the bioactivity of ZnO and CuO nanoparticles in a soil bacterium. *Environ. Pollut.* **2014**, *187*, 65–72. [CrossRef] [PubMed]
98. Ullah, S.; Adeel, M.; Zain, M.; Rizwan, M.; Irshad, M.K.; Jilani, G.; Hameed, A.; Khan, A.; Arshad, M.; Raza, A.; et al. Physiological and biochemical response of wheat (*Triticum aestivum*) to TiO_2 nanoparticles in phosphorous amended soil: A full life cycle study. *J. Environ. Manag.* **2020**, *263*, 110365. [CrossRef] [PubMed]